Investigating Laser Control over Crystal Nucleation

Nina L. H. Kinney

Submitted in fulfilment of the requirements for the
Degree of MSc by Research

School of Chemistry
College of Science and Engineering
University of Glasgow

October 2020

Abstract

The aim of this project was to investigate the incidence of femtosecond laser-induced crystal nucleation in various compounds, setting the results in context. The search for greater understanding of the mechanisms underlying non-photochemical laser-induced nucleation (NPLIN) and better control over nucleation processes are highly sought after. The following work details the study of laser-induced crystal nucleation in solutions of potassium chloride, glycine and lysozyme to date. Through a comprehensive critical review of the relevant literature, supplemented by an experimental investigation of NPLIN in KCl solutions, the strength of evidence for possible mechanisms underlying this enigmatic phenomenon will be evaluated.

From an overview of the relevant literature, it is clear that evidence for opposing theories of nucleation is developing in parallel, indicating that the existence of multiple mechanisms is likely. The nature of these mechanisms, and factors governing the prevailing mechanism for a given system, leaves much to be explored. This report will contrast observations, in order to shed some light on opposing theories and to identify inconsistencies, where further study is needed.

Experimentally, it was found that femtosecond laser irradiation could successfully induce crystallisation in KCl/D_2O solutions. The likelihood of NPLIN occurring was found to depend on the saturation value, as expected, and also the laser power. Higher laser powers (with approximately 0.8 W – 1 W reaching the sample droplet) were found to consistently produce vapour bubbles in heavy water solutions, despite low absorption due to molecular vibrations. The observation of laser-induced bubble formation could be considered an indication that the NPLIN demonstrated resulted from nano- or micro-bubble formation and collapse, as oppose to laser trapping.

All this aims to establish a concrete starting point for the CONTROL project, which seeks to build greater understanding of laser-induced nucleation, with particular emphasis on the consideration of laser-induced liquid-liquid phase separation as a possible precursor to crystal nucleation.

Contents

List of Tables

List of Figures

Acknowledgements

Firstly, I would like to thank my supervisor Professor Klaas Wynne for his support and guidance – particularly through such difficult circumstances.

I would like to express my gratitude to Dr Zhiyu Liao for his very valuable help with the optics side of the experiments before the lab was shut down, and to Dr Mario González Jiménez for so kindly sharing his lab wisdom throughout the year. I would also like to thank other past and present members of the Wynne Lab: John Bolling, Andrew Farrell, Dr Ben Russell, Dr Chris Syme, Dr Finlay Walton and Elen Williams for all of their help and company.

Finally, I wish to thank my family and friends for their love and support – throughout this year and always.

Declaration

I confirm that the work contained in this thesis, submitted for the degree of Master of Science, is a result of my own work except where explicit reference is made to the contribution of others. No material within this thesis has been previously submitted for any other degree at the University of Glasgow or any other institution.

Nina L. H. Kinney
15th February 2021

List of Abbreviations

CNT	Classical Nucleation Theory
CW	Continuous Wave
FTIR	Fourier Transform Infrared
HEWL	Hen Egg White Lysozyme
LIN	Laser-Induced Nucleation
NIR	Near Infrared
NLIN	Non-photochemical Laser-Induced Nucleation
OKE	Optical Kerr Effect

Chapter 1

Introduction

1.1 Nucleation

Nucleation is the *first step* in the formation of a new thermodynamic phase. The appearance of bubbles in a glass of champagne, condensation in clouds, and the crystallisation of caramel are all common examples of evidence for nucleation. There are numerous cases of nature itself utilising nucleation phenomena: from atmospheric fungal spores influencing cloud behaviour [4] to antifreeze proteins in fish [5]. For such a ubiquitous process, surprisingly little of the chemical physics underlying nucleation is well understood today.

In this report, the term 'nucleation' will refer primarily to the first step in the formation of crystals from liquid solution. The process of crystal formation can be understood as consisting of two steps: nucleation followed by growth. The time taken for the nucleation step dictates the kinetics of crystal formation.

Over the years, investigations have shed some light on aspects of nucleation phenomena – highlighting factors which influence the behaviour and possible mechanisms. But nucleation is a complex problem. There are inherent experimental difficulties in its characterisation, due to its scale and speed (by definition nucleation is the stage before we see anything happen) and because nucleation itself is a fundamentally stochastic phenomenon. Computationally, ambiguity in modelling nucleation is unavoidable because the mechanism and influences are not yet known.

A number of conceivable mechanisms have been proposed; yet there is not one theory which fully explains all the phenomena we observe. This lack of understanding on the underlying mechanisms is preventing progress to greater control of nucleation phenomena.

1.1.1 Some Terminology

Primary nucleation describes the birth of a new crystal from a uniformly liquid phase. Secondary nucleation, on the other hand, describes the formation of new crystals where parent crystals are already present in the solution, as in a continuous crystallisation process. There is considerable evidence to show that the energetic barrier to secondary nucleation is reduced, in comparison with that of primary nucleation. Current scientific and industrial crystallisation challenges – such as pharmaceutical production and the nucleation of hard-to-crystallise proteins – are rooted in the lack of control over primary nucleation. Greater control over primary nucleation times and polymorph selectivity would be of extensive value. For this reason, this report will focus on investigating primary nucleation phenomena.

Another important distinction is that of heterogeneous and homogeneous nucleation. The most common form of nucleation is heterogeneous [6] – that is a crystal forming on a foreign surface such as an impurity particle or interface. An example of evidence for heterogeneous nucleation of KCl crystals is shown in Figure 1.1.

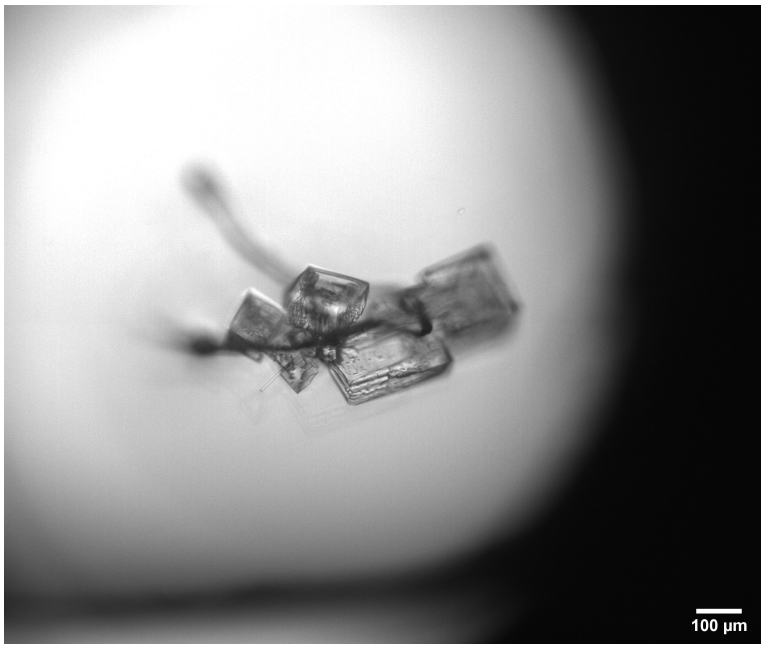

Figure 1.1: Evidence of heterogeneous nucleation – crystals of KCl growing on a thread in a droplet. Picture taken 06/03/2020.

Homogeneous nucleation occurs in the absence of foreign surfaces. Experimentally, homogeneous nucleation is challenging to study. While evidence for nucleation can be detected by crystal growth, it is practically impossible to remove the possibility that the nucleation

detected was heterogeneous. Modern methods for studying homogeneous nucleation often utilise purified chemicals and nanoscale filtration, to remove impurity particles and reduce the likelihood for heterogeneous nucleation.

1.1.2 Classical Nucleation Theory for Homogeneous Nucleation

Classical Nucleation Theory (CNT) is the most well known quantitative theory of nucleation. CNT is grounded in the work of many scientists, primarily Gibbs [7], Volmer and Weber [8], Becker and Döring [9] and Frenkel [10]. There are examples of where CNT fails to describe what is experimentally observed [6] [11] and new theories have been put forward in response. Still, many of these incorporate elements of the classical theories.

CNT provides an explanation for the evolution of fluctuations in a metastable solution. The constant motion of particles in solution will result in random collisions and the formation of molecular clusters, or nuclei. Occasionally, these collisions will result in the formation of a critical nucleus – that grows to form a crystal.

$$\Delta G = 4\pi r^2 \gamma + \frac{4}{3}\pi r^3 \rho \, \Delta\mu \tag{1.1}$$

In Equation 1.1, ΔG is the free energy change for nucleation, γ is the interfacial tension between nucleus and solution, ρ is the number of molecules per unit volume in the solid and $\Delta\mu$ is the difference in chemical potential between the solid and liquid phases (this term is negative in a supersaturated solution). Finally, r is the radius of the nucleus; hence $4\pi r^2$ and $\frac{4}{3}\pi r^3$ are its surface area and volume, respectively, assuming the cluster forms a spherical shape to minimise the surface to volume ratio.

The equation for the homogeneous nucleation barrier, ΔG, simply describes the outcome of nucleus formation, growth or dissolution, as an energetic contest between two terms: the energetic barrier to the formation of a solid-liquid interface (r^2 term) and the free energy reduction of growing the bulk solid, where this is the most thermodynamically stable phase under the conditions of the metastable state (r^3 term). These opposing terms can be visualised as in Figure 1.2. Differentiating the equation for homogeneous nucleation with respect to r gives r_c, the critical radius. This is the minimum size of the nucleus such that it becomes energetically favourable for nucleation and growth to occur.

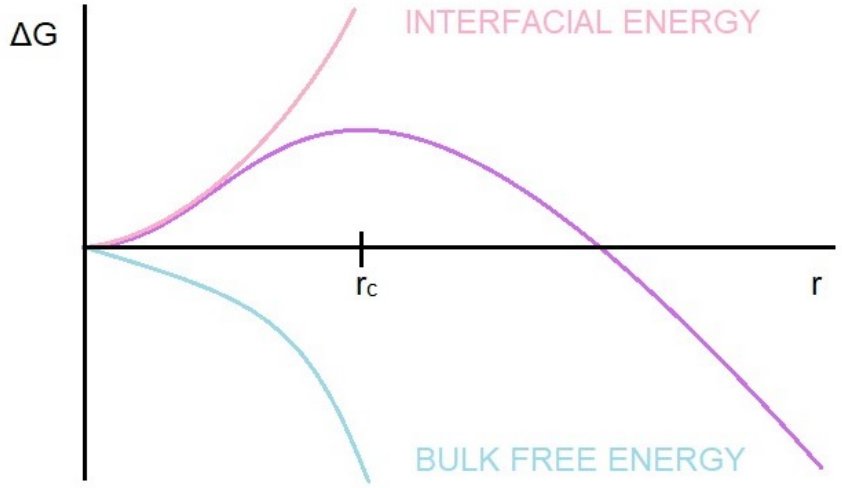

Figure 1.2: Free energy, ΔG, vs cluster radius, r. Illustrating two opposing energy terms and their sum. The critical radius, r_c, is indicated.

1.1.3 Saturation and Stability

The saturation value, S, is an important quantity when investigating nucleation in simple solutions, such as salts or amino acids. The saturation is calculated by $S = C/C_{\text{sat}}$ where C is the concentration of the solution and C_{sat} is the solubility of the solute in the solvent. The degree of saturation dictates the stability of the solution with respect to nucleation. When a solution is supersaturated, the chemical potential for a solid will be lower than that of the solution [12] – it is said to be *metastable*. In this state, crystal formation is thermodynamically favourable, but the kinetic barrier to nucleation can prevent solid forming. There are experimentally demonstrated methods that seemingly reduce this kinetic barrier to nucleation and can induce spontaneous crystallisation in metastable solutions such as sonocrystallisation, mechanically-induced nucleation, and laser-induced nucleation.

The degree of supersaturation also affects the rate of crystal growth and hence the quality of crystals formed. Moderate supersaturations combined with external stimuli to induce nucleation are preferable for obtaining large, well-formed crystals because the subsequent growth will be relatively slow. Highly supersaturated solutions are more susceptible to incurring multiple nucleation points resulting in smaller, poor-quality crystals, as solute is rapidly precipitated out.

Developing the theory for nucleation phenomena has broad implications, extending far

beyond understanding the intrinsic science. From protein crystallography to pharmaceutical development, crystal nucleation is of fundamental importance to science and industry. Thus, there is a practical aim in investigating the conditions which inhibit or promote nucleation in various substances – as it offers potential to gain highly valuable control over what is a fundamentally stochastic process.

1.2 Inducing Nucleation with Light

Photochemically induced nucleation was first recorded by John Tyndall in 1869; he described in detail light-induced chemical reactions in vapour forming a condensed phase [13]. In 1996, Garetz et al. reported on the laser-induced nucleation (LIN) of supersaturated solutions of urea [14]. On account of the transparency of urea solution at the incident wavelength, the observed crystallisation was evidently occurring by some physical mechanism, without inducing photochemical reaction, and so was termed non-photochemical laser-induced nucleation (NPLIN). This was an exciting discovery; not only did it imply a new means for controlling nucleation by light, but it opened up a new route of investigation to a better understanding of the underlying mechanisms for nucleation itself.

Since then, nanosecond-pulsed NPLIN has been demonstrated for many simple systems from salts such as KCl [15], NH_4OH [16] and NaOH [17] to acetic acid [18] and glycine [19]. A number of mechanisms have been proposed to account for this type of nucleation. From the laser-induced alignment of molecular clusters to the heating of impurities producing micro-bubbles; it is possible that one or many of these suggested mechanisms can occur.

1.2.1 Laser-Tweezing Crystals from Solution

A variant of NPLIN using continuous-wave (CW) or femtosecond-pulsed laser light, as opposed to nanosecond-pulsed, has also now been demonstrated. The most prolific testimony of this effect concerns the crystallisation of protein solutions. While this report will consider NPLIN more generally – it is important to distinguish between NPLIN methods – since it is now broadly accepted that nanosecond and femtosecond/CW nucleation are likely to occur via different physical processes. A complete overview and discussion comparing results for nanosecond, femtosecond and CW NPLIN in various systems is lacking and the mechanisms not yet fully understood. The behaviour of a solution exposed to laser light will depend on various factors, including pulse rate and composition. Experimental comparisons serve to better elucidate the underlying physics, where there is a lack

of consensus in findings.

Femtosecond or CW induced nucleation is generally understood to occur by some form of optical trapping, which has been extensively demonstrated for larger particles (e.g. glass beads) in solution, using femtosecond and CW lasers. Optical trapping is a well-known phenomenon, first demonstrated in 1970 [20], in which higher-refractive-index objects are drawn into the focus of the laser beam by electrical gradient forces.

It has been stated that femtosecond-pulsed laser irradiation can be considered similar in terms of trapping effect of solid particles to CW irradiation [21], and possibly even more effective in some cases [22]. Both types have been used successfully in previous primary nucleation studies. However, the details of exactly how this crystallisation manifests in pure liquid solutions remain unclear. It has been suggested that some combination of particle trapping, heating and controlled diffusion by laser irradiation may be important – as these could aid cluster alignment or generate highly supersaturated regions where nucleation is more likely.

1.2.2 The Separation of Liquid Phases

For some time it has been thought that fluctuations occurring in the region close to liquid-liquid critical points may reduce the energy barrier to crystal formation [23]. A more recent study suggested, by molecular dynamics simulations, that despite crystallisation rate increasing with the formation of a dense liquid phase, there was no particular advantage of proximity to metastable critical points [24]. Yet, it has since been shown that femtosecond laser irradiation can be used to induce concentration gradients and bring about the separation of liquid phases directly [25] [26].

In their recent publications, Walton and Wynne focus specifically on the phase separation of a liquid mixture, as opposed to the nucleation of crystals. However, the theory underlying their discovery may also be applicable for the nucleation of crystals from solution. It is well known that many compounds have liquid-liquid critical points, though they are often hidden. It has even been suggested that all liquids may contain these points, and they may play a key role in crystallisation.

Figure 1.3 illustrates the important concepts underlying this idea – the main objective being to uncover the relation between the supposed liquid-separation curve (shown in (b)) and the observed nucleation by action of the laser (indicated in orange in (a)).

According to CNT, the probability of crystal nucleation depends on the degree of solution

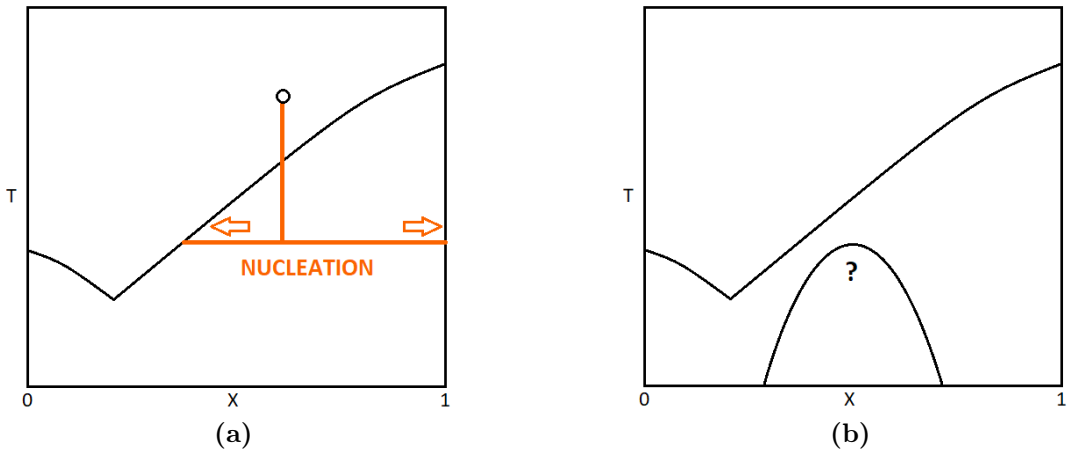

Figure 1.3: Phase diagrams highlighting the key features of a new approach to understanding femtosecond LIN phenomena: (a) laser-induced phase separation shown in orange and (b) the unknown proximity of a liquid separation curve.

saturation, so it follows that an external action to influence local concentration, and capable of inducing the separation of liquid phases near a liquid-liquid binodal, could offer a means of promoting crystallisation. However, obtaining a detailed understanding of liquid phase behaviour in relation to NPLIN is clearly a huge challenge. The role of liquid phase separation in the observed femtosecond/CW induced crystallisation and the link to nanosecond nucleation remains unclear.

The novel approach presented by Walton and Wynne, primarily focusing on liquid-liquid phase separation as a precursor to crystal formation, presents an alternative route to understanding the reported incidence of rapid-pulse induced crystallisation. In contrast to previous studies, the development from laser-induced separation of liquid phases to crystallisation, if successful, would provide a more complete picture of the dynamics responsible and a clear opportunity for manipulation.

1.2.3 Crystal Nucleation

From the literature and experiments it is appearing increasingly likely that there are in fact multiple photophysical routes to promote nucleation by laser light. The demonstration of liquid phase separation by laser irradiation is undoubtedly a significant finding, and in this report it will be shown that femtosecond laser irradiation can also be used to induce crystallisation in KCl/D_2O solutions using the same experimental set-up. However, the extent to which this NPLIN is accounted for by trapping phase separation effects is still

unknown.

NPLIN is a useful model for investigating homogeneous nucleation as crystallisation can be induced in a pure and sealed system. The challenge of developing this technique for applications in more hard-to-crystallise systems is held up by the lack of understanding of the underlying mechanisms. Hence, the searches for control and understanding of nucleation are coupled. While the pursuit of a theory that completely describes nucleation phenomena continues, there is benefit to be sought from continuing research attempting to uncover the mystery of nucleation from different points of view. While nanosecond NPLIN phenomena have been more extensively studied, more recent observations of femtosecond and CW NPLIN have been considered quite distinctly and investigated to a lesser extent.

Chapter 2

Mechanisms for NPLIN

There are two main approaches to understanding the basis of mechanisms for nanosecond-pulsed NPLIN; with a further optical trapping based approach to CW and femtosecond NPLIN. The bases of these are outlined in the following sections and are discussed further throughout the report.

2.1 Dielectric Polarisation

From the first observations of NPLIN in urea it was initially suggested that NPLIN may be occurring by a nonlinear optical Kerr effect (OKE) mechanism [14], in which an electric field induces the alignment of molecules. This description was consistent with the authors' observation that crystallites of urea appeared to have aligned preferentially along the plane of polarisation. This observation was later discredited by Alexander, who imaged laser-induced crystallisation in urea, showing no significant correspondence between the alignment of linear polarisation and urea crystals [27]. Computationally, simulations predicted that optical Kerr interaction energies would not be sufficient to induce nucleation [28]. On top of this, the nucleation of salts, like KCl, seemed to follow the same behaviour despite there being no such molecular units in solution to align [29].

Other related mechanisms were soon proposed. For example, the isotropic electronic polarisation method based on the polarisation of precursor clusters. This is a two-step mechanism, referred to as a modified CNT model [12]. By this method nucleation is described as diffusion-controlled cluster formation, followed by the structural reorganisation of the clusters by laser light.

There is some evidence that the electrical-field-induced alignment plays a part in reducing the energy barrier to nucleation – particularly given the observed correlation between polarisation and formation of specific crystal polymorphs (see Section 4.1). However, there are articles that dispute this in the case of nanosecond-pulsed NPLIN, where the reported correlation has proved difficult to replicate, so results are inconsistent.

One of the main problems cited with polarisation mechanisms for NPLIN is their lack of explanation for repeatedly observed power thresholds. Mechanisms based on laser heating, on the other hand, better account for these observations [27].

2.2 Cavitation and Pressure Waves

In response to the inconsistencies with proposed polarisation mechanisms, others have considered the role of bubbles in NPLIN, as another possible route to crystallisation. Mechanical shock and exposure to ultrasound are well known to be capable of inducing nucleation in metastable solutions. While the underlying mechanisms are not well understood, present understanding is based on the transient formation of saturation gradients due to induced high-pressure zones [30]. The production of bubbles by ultrasound has also been demonstrated and it remains unclear whether nanocavitation, and the brief formation of an air-liquid interface, is key to inducing nucleation in these instances, or whether pressure waves are themselves sufficient.

The LIN of CO_2 bubbles in carbonated water has also been demonstrated [31] [32]. It was reported by Knott et al. that laser irradiation could successfully induce vapour bubble formation in carbonated water [31]. Additionally, in water supersaturated with both argon and glycine, bubbles produced by pressure release were subsequently found to induce crystal formation – establishing a possible connection between the formation of bubbles and crystals in NPLIN. A supersaturation dependent power threshold, similar to that recorded for NPLIN, was found to exist for laser-induced bubble formation. Interestingly, variations between carbonated ultrapure and tap water samples were found to be negligible, suggesting the effect of impurities was insignificant, contrary to observations recorded in other NPLIN studies.

Ward, Mackenzie and Alexander attribute the production of CO_2 bubbles, in their study, to the laser heating of nanoparticles [32]. These vapour bubbles, according to CNT, can reach a critical radius and then grow. It is also suggested that the NPLIN of crystals may occur by a similar pathway. Surprisingly, Ward et al. also report that no bubbles were observed with unfocused femtosecond-pulsed irradiation, even at high peak power densities [32];

perhaps further evidence that the nanosecond and femtosecond NPLIN occur by different means. Although, as discussed later in this report, our own observations may indicate otherwise.

In 2007, Nakamura, Hosokawa, and Masuhara found a direct link between laser-induced bubble formation and crystallisation in anthrocene by a single femtosecond laser pulse [33]. In this paper, the authors fail to provide a clear account of the full mechanism but they do consider some potentially important effects, such as cavitation and collapse, from thermal expansion due to multiphoton absorption; ultimately attributing the bubble formation to "several non-linear effects". It is interesting that the authors acknowledge another study confirming the crystallisation of lysozyme at the surface of laser-induced bubbles and yet insist that this mechanism is entirely distinct from that based on the optical field. Considering that the same authors have published accounts of laser trapping crystallisation (many of them using lysozyme), it is unclear how these two potential mechanisms may align.

Nakamura et al. do not elaborate further on the mention of multiphoton absorption. While this has not been directly discussed in the other literature either, it is suggested that a broader investigation of wavelength dependence is necessary to completely dismiss a photochemical mechanism [31]. Ward et al., argue that a photochemical mechanism is unlikely, from their observations of nanosecond LIN of simple salts. They also state that laser absorption leading to bubble formation and collapse could still reasonably be called non-photochemical [16]. In most cases of 'NPLIN' it is unclear what photochemical process could possibly be occurring, so for the purposes of distinguishing these phenomena from clearly photochemical experiments it does makes sense to label them differently.

The formation of transient nano- or micro-bubbles could potentially catalyse crystal formation in NPLIN without being detected, either by providing heterogeneous nucleation sites or inducing pressure gradients on collapse. However, at this point it remains quite unclear why the bubbles are produced in the first place (which may differ from substance to substance), and to what extent their undetected presence is responsible for observations of NPLIN.

It is thought that the heating of particles in nanosecond pulsed NPLIN may induce high-energy cavitation or pressure waves, prompting crystallisation. In fact, the increased proclivity to form the γ-glycine polymorph with increasing supersaturation is explained in terms of this mechanism (see Section 6.2) on account of the similarities in the results for NPLIN with nucleation by mechanical shock and sonication (both understood to result from cavitation).

2.2.1 Nanoparticle Heating

The role of impurity nanoparticles in nanosecond NPLIN of ammonium chloride solutions is discussed in depth by Ward, Mackenzie and Alexander [16]. In this paper, the authors discuss results and implications regarding proposed mechanisms. Primarily, they find that 0.2 μm filtration significantly reduces the likelihood of NPLIN by nanosecond laser irradiation. They identify impurities in the filter residue, by inductively coupled-plasma optical-emission spectroscopy and mass spectrometry, to be predominantly iron and phosphate. Finally, by intentionally doping pre-filtered solutions with iron oxide nanoparticles, the incidence of NPLIN in these solutions was found to be similar to that of the unfiltered solutions – suggesting the presence of impurity particles as opposed to simply large clusters of solute may have some role in the mechanism. Dynamic light scattering measurements revealed the presence of $\approx 1\,\mu$m diameter particles in unfiltered solutions, which the authors suggest may be solute structures surrounding smaller impurity particles.

It is argued that a nanoparticle heating mechanism, by contrast to the polarisability mechanism, justifies the observation of power thresholds for crystal nucleation. This is because solvent evaporation may rely on a critical threshold temperature being reached. Some other observed effects, such as the reluctance of certain compounds to undergo NPLIN, can also be explained by the nanoparticle heating mechanism, on account of the presence (or lack of) specific impurities.

It has been widely established that the nano-filtration of solutions effectively suppresses NPLIN in liquids. However, it remains unclear exactly why this is the case and there is at least one example where the presence of impurities made no significant difference to the results [31]. Filtration effects are therefore an important consideration for future NPLIN studies. The main counterpoint to a nanoparticle heating based mechanism results from observations of polarisation effects. Polarisation switching by nanosecond irradiation has been somewhat discredited by its lack of replicability; yet polarisation effects have also been recorded for CW NPLIN of glycine [34].

Although ultimately the literature does demonstrate a clear connection between laser-induced nucleation of bubbles and crystals, there is a lack of consensus on the details maintaining the mystery of such a mechanism. Contrasting observations in the literature such as the failure [32] and success [33] of femtosecond irradiation to produce bubbles and the apparent differing significance of impurity particles' presence [31] [16] leave much to be explored.

2.3 Laser Trapping

In recent years, demonstrations of crystallisation by femtosecond and CW NIR laser light have suggested other possible pathways to nucleation. In 2003, Adachi et al. published a paper describing experiments utilising femtosecond pulse rates at a wavelength of 780 nm to generate crystal nuclei in microlitre lysozyme droplets, under conditions where spontaneous nucleation would not usually occur [35]. The authors offer a limited explanation of this effect as a result of high peak intensity femtosecond laser irradiation "nonlinear nucleation processes". Since then, variations on the same technique have been used in the crystallisation of lysozyme [36] [37] and glycine [38] [39] [40]. Most astonishingly, laser-induced crystallisation in *undersaturated* solutions of glycine/D_2O has since been reported [41] – these experiments are discussed further in Section 4.2.3.

Tsuboi et al. describe the formation of a lysozyme aggregate – identified by backscatter imaging and Raman microspectroscopy – formed by photon pressure in the laser focus [36]. They find that CW irradiation, on a timescale of 1-2 hours, can effectively trap lysozyme clusters of <10 molecules in the beam and that these areas of increased concentration can serve to promote crystal growth. This is the first meaningful evidence that laser trapping can apply to protein clusters in solution and that some form of laser trapping may function to trigger crystallisation. The authors found an increased proclivity to nucleate crystals after 24 hours in the irradiated samples. It is not entirely clear from these experiments alone whether protein aggregation (by laser trapping) is a prerequisite to CW crystallisation, and which factors may determine the likelihood of a crystal forming if so. However, the results are a promising step in the search for greater control.

Interestingly, Tu et al. discuss influencing crystal growth by laser trapping close to a spontaneously formed crystal [42]. They propose a mechanism for laser trapping-induced protein crystal growth, involving two distinct domains with different liquid-like cluster arrangements induced by laser irradiation. Although this is a considerably different process to NPLIN, the effects confirm that laser trapping in solution can induce concentration gradients, affecting the dynamics of crystal growth in lysozyme.

Lee et al. examine the effects of laser intensity, wavelength, and pulse duration on nucleation probability in irradiated lysozyme droplets. Their observations lead the authors to conclude that NPLIN is promoted in lysozyme solutions by concentration fluctuations due to mixing and occurs by some "electric-field-induced reorganisation" [37]. They suggest that further study is required to elucidate such mechanisms fully.

It is clear from these reports that even within femtosecond/CW nucleation experiments

there lacks a full understanding of the mechanism, while it has been widely acknowledged that this is likely to differ from that of nanosecond NPLIN. There is some consensus in the literature that this nucleation occurs by a two step process – the first step being some form of aggregation or density fluctuations and the second being structural re-ordering by action of the laser. However, more recently, even this belief has been challenged by demonstrations of laser-induced bubble formation in protein solutions (see Section 5.4). Undoubtedly, further investigation is needed to identify the mechanistic significance of these behaviours, and to establish whether they are a feature of the solutions studied or something more general.

Chapter 3

Nucleation of KCl

Aqueous solutions of potassium chloride have been used frequently in studies of nanosecond NPLIN. In fact, it has been stated that KCl solutions are some of the most labile with respect to laser-induced nucleation [43]. The relative simplicity of these salt solutions provides an opportunity to gain direct insight into the nucleation process. Despite this, there are no known examples of CW or femtosecond studies of NPLIN of KCl (probably due to the assumption that laser trapping crystallisation is only successful in the trapping of larger molecular clusters). Some preliminary experiments of this kind are detailed later in the report (see Section 9).

3.1 NPLIN of KCl

NPLIN of aqueous supersaturated solutions of potassium chloride, by single nanosecond pulses of 1064 nm laser light, was first demonstrated by Alexander and Camp in 2008 [15]. In this study, the laser power and supersaturation required for NPLIN were measured in repeated experiments. Notably, this paper describes the laser-induced formation of a single crystal of KCl, with increased concentrations and laser powers yielding more than one crystal. This provides some indication of the degree of control obtainable through such techniques. The possibilities for temporal and spatial control of nucleation have been further demonstrated with controlled crystallisation of KCl in agarose gels by NPLIN [44]. It is clearly shown in this case, due to the reduced currents in gels, that despite the stochastic nature of nucleation, crystallisation by NPLIN is limited to the location of the laser focus.

A threshold peak power density (MW cm^{-2}), below which solutions would not crystallise,

has been identified for KCl, both in gel [44] and in aqueous solution [15] [45]. Above this, experiments have shown that the number of crystal nuclei formed is linearly dependent on peak laser power density [46]. An explanation for the threshold power for NPLIN has not yet been identified. Though, accordant threshold power density values were found for supersaturated aqueous KCl droplets levitated in an electrodynamic trap [43] – discounting the possibility that the power threshold may be associated with the sample containers. This highlights a key area for further investigation, as the nature of the power threshold is unknown. While results from various experiments using nanosecond pulsed lasers for NPLIN of KCl have produced consistent results for threshold powers, the relation between CW and femtosecond NPLIN results remains to be seen.

3.1.1 Wavelength and Temperature Effects

The levitated droplet study by Fang et al. successfully demonstrated NPLIN of aqueous KCl droplets using 532 nm nanosecond pulses. The effect of wavelength and temperature has been investigated in some detail for NPLIN of KCl and KBr [46]. In fact, the threshold power value was found to be lower for 532 nm irradiation than for 1064 nm, for NPLIN of halides, in a similar trend to that observed in urea solutions. Fang at al. attribute the increased NPLIN efficiency at 532 nm to corresponding lower water absorption coefficient compared with that of 1064 nm [47].

Increased absorption at 1064 nm, due to vibrational overtone absorption at this wavelength [41], will mean greater localised heating with laser irradiation. This could hinder nucleation as it effectively decreases the local supersaturation in the laser focus. The absorption of solvents is an important consideration for NPLIN, particularly with sustained irradiation. For this reason, the substitution of D_2O for H_2O is common in femtosecond/CW NPLIN studies, due to its reduced absorption at 1064 nm. Yet, Ward and Alexander find the temperature variation caused by laser irradiation to be negligible in their case, where *single* nanosecond laser pulses at reduced power densities are used to induce crystallisation [46]. They estimate the temperature change on irradiation to be only a fraction of a degree and yet still observe the same wavelength-dependent trend. All this gives some indication of the complexities involved in understanding the mechanisms responsible and, in particular, how laser heating may affect various forms of NPLIN.

In contrast to previous findings, a more recent study by Kacker et al. states clearly that no dependence on the laser wavelength with unfocused nanosecond NPLIN, at 355 nm, 532 nm and 1064 nm is observed [48]. However, results presented in the same paper do appear to show that, at lower intensities, the probability for nucleation is higher at shorter

wavelengths (355 nm > 532 nm > 1064 nm). Perhaps these results were considered too inconsistent by the authors to confirm the trend. This study does highlight the necessity to account for the stochastic nature of nucleation by using a large number of samples. This type of analysis is essential in nucleation investigations to achieve certainty, where variations in outcome from sample to sample can be significant, and often entirely random. Nevertheless, and while further experimentation may be required to reach an explanation, Kacker's results certainly do also demonstrate some wavelength dependence of NPLIN, in agreement with previous studies. It is odd that the authors explicitly state no wavelength dependence at the outset and offer no further analysis. As previously stated, the origin of the apparent power threshold for NPLIN is not yet known; however developing knowledge of the features of NPLIN – such as the apparent wavelength dependence – is useful in the pursuit of a complete explanation.

3.1.2 Observations on Mechanism

Filtration of samples has been found to reduce the probability of nucleation in KCl solutions [48]; while measurements of diffusion coefficient showed a decline with increasing KCl concentration in the supersaturated region – indicating cluster formation [49]. In addition, a computational study of aqueous KCl, discussed in the context of NPLIN*, found evidence of electronically polarisable clusters with a relaxation time corresponding to the laser pulse duration used by Alexander in previous experiments ($\approx$ 100 ps) [50]. All this seems to support the dielectric polarisation method, yet fails to account for the apparent power threshold.

It is stated in this paper that experimental observations by Alexander and co-workers suggest a laser pulse duration of less than $\approx$ 5 ps will not induce nucleation, even at high intensities [50]. Our own observations indicate that a high repetition rate femtosecond pulse train can induce nucleation of KCl. However, the mechanism and details of femtosecond-pulsed NPLIN in KCl solutions remain elusive.

Interestingly, a study on the pulse width dependence of NPLIN in KCl solutions found the fraction of samples nucleated by 6 ns and 200 ns irradiation was the same [51]. It is concluded by the authors that the nucleation probability depends directly on peak-power density but not necessarily on pulse width or total energy. The authors note that (non-KCl) studies using shorter pulsed lasers would correspond to significantly higher peak powers and crystallisation may therefore occur by a different photomechanical process,

*It is important to note that while computational studies are extremely useful to complement experiments, NPLIN itself cannot yet be modelled by molecular dynamics simulations because the characteristics of these light matter interaction are unknown.

which seems likely.

3.1.3 Experimenting with KCl

Most recently, a microfluidic device was used to characterise nucleated crystals, finding the threshold peak power densities in agreement with those of Alexander and co-workers [45]. These experiments exemplify the use of controlled thermoelectric cooling to achieve supersaturation in solutions. This is one alternative method to the batch analysis of glass vials, where the preparation and storage of samples can be laborious due to the tendency for supersaturated solutions to nucleate spontaneously. It is well known that nucleation can be induced mechanically, so even the slightest vibration or disturbance of the sample container can induce nucleation before experiment. This renders samples unusable for primary nucleation studies with NPLIN and effectively decreases the supersaturation of solutions as KCl is precipitated out. For this reason the preparation of samples for testing is one of the main practical challenges in nucleation studies.

It was noted that a significantly increased saturation value, $S = 1.2$, was required for nucleation of picolitre droplets of KCl/H_2O solution compared with $S \approx 0.6$ in bulk solution. These results were used to inform the experiments outlined in this report and are discussed further in Section 6.1. This effect was attributed to a lower nucleation rate as a result of smaller droplet volume – accounted for in terms of the isotropic electronic polarisation method for nucleation. This method enables calculation of the rate of formation of subcritical solute clusters in the irradiated sample volume, assuming that the supersaturation dependence according to CNT still holds, as observations suggest. Additionally, the solubility of KCl in D_2O is such that the saturation value, S, can be brought within the region required for inducing NPLIN by cooling a solution made up to be undersaturated at room temperature for ease of handling (see Section 6.1 for more details). For this reason, KCl was elected as a primary candidate for our own investigations.

It has been highlighted that the nanosecond pulsed NPLIN experiments should not be compared directly to femtosecond nucleation studies [15]. Femtosecond pulses are more powerful in that their pulse energy is delivered over a shorter time. Previous nanosecond studies of KCl are therefore useful as a reference but could not be used to predict the outcome of femtosecond NPLIN in KCl – as it could likely occur by an entirely different mechanism, if at all. This is important to bear in mind during the discussion of KCl experimental results.

Chapter 4

Nucleation of Glycine

Glycine is the simplest amino acid and exists as a zwitterion ($^{+}NH_3CH_2COO^{-}$) dissolved in pure water [19]. Investigations of amino acids can be useful as model systems in the development of understanding the behaviour of more complex biomolecules, such as proteins. Glycine itself has been selected for a number of nucleation studies, which have investigated NPLIN in glycine solutions and crystal polymorphism.

4.1 Polymorphism

Glycine is a particularly interesting system in that it has three crystal polymorphs obtainable under normal laboratory conditions (α, β, and γ), with three further polymorphs discovered at high pressures (δ, ϵ and ζ) [52] [53]. These polymorphs, or different crystalline forms, can differ in their chemical and physical properties e.g. reactivity, melting point and solubility [54]. Consideration of polymorphic activity in vivo is therefore crucially important in drug design [55] [56]. As such, and in particular for pharmaceuticals, there is a need for greater understanding of the conditions that influence polymorphism. Polymorphs can be notoriously hard to pin down, and have appeared to exhibit strange sensitivities, such is the phenomena of the disappearing polymorph [57]. Hence, the ability to predict and to control the formation of a desired polymorph is highly sought after.

In the case of glycine, the polymorphs differ by their arrangement of zwitterions. The α-form consists of discrete double-layers of zwitterions. The β- and γ- forms are 3D networks linked by H-bonds, with zwitterions arranged in individual layers and helices, respectively [58]. Powder X-ray diffraction is often used to distinguish between polymorphs. While visual inspection of the crystals formed can provide some indication as to the polymorphic

structure [59] – bigger translucent crystals have been identified as α-type and thin needle-like crystals and smaller opaque crystals as γ. What is typically referred to as 'glycine' is commonly a mixture of α- and γ- forms [58].

The thermodynamic stability of each of these polymorphs will depend on conditions such as temperature and pressure. It is also crucial to note that the rate of transformation from one polymorph to another can vary greatly; the conversion from a less stable polymorph to a more stable polymorph can be indeterminately slow [60]. So there are at least two important considerations when discussing polymorph stability: thermodynamics and kinetics. The time-frame for transition to a thermodynamically stable state will be determined by the transformation kinetics, related to the liquid structure.

One factor known to impact polymorphism is the degree of solution saturation. These effects are discussed in more depth in Section 6.2, where it is highlighted that reports of an increased tendency to form γ-glycine from heavy water solutions fail to acknowledge aqueous solubility differences. For this reason, it seems likely that this observation is equivalent to the finding that at higher supersaturation the formation of γ-glycine is more prevalent [30]. However, the observation of a transformation from *deuterated* α- glycine powder to γ- at room temperature (where no such transition otherwise occurred) is very interesting [61]. This is undoubtedly an area due further investigation.

4.2 NPLIN of Glycine

The first record of NPLIN studies of glycine was published in 2000 by Zaccaro et al. [19]. This paper places emphasis on the laser-induced formation of γ-glycine by NPLIN as opposed to α-glycine – most commonly formed by spontaneous nucleation. The results are presented simply; however further analysis suggests there may be more subtle factors involved in this apparent bias. According to Zaccaro et al. the α-polymorph is "known to be the most stable" of the three forms, from stated observations that β- and γ- polymorphs will spontaneously transform to α where mother crystals of the α-form are already present in solution [19]. Yet, according to thermodynamic studies of these polymorphs, the behaviour of glycine is far more complex than this suggests [58]. It is true that the α-polymorph is the most likely to form on spontaneous nucleation of a saturated solution under ambient conditions. However, it is not the most *thermodynamically stable* – it is the kinetically favoured form (see Section 4.2.1). It has been found that the α-form will convert to the most thermodynamically stable γ-form after some time. The confusion and inconsistencies with thermodynamic stability in the literature are unsurprising, considering that crystallisation experiments often favour different polymorphs for obscure

reasons.

4.2.1 Ostwald's Rule of Stages

The initial formation of a less stable polymorph is surprisingly common in nature. This observation was first made in 1897, later termed 'Ostwald's Rule of Stages' [62]. In this early work, Ostwald discussed crystallisation behaviour, polymorphism and stability of solutions. Remarkably, he reasoned that the crystal phase formed under certain conditions will be that closest to the liquid in free energy, not the most thermodynamically stable [63]. This is initially surprising, since according to macroscopic thermodynamics the new phase formed should be the lowest in free energy [11]; however, experimental observations suggest this outcome is rare.

The preferential formation of the least stable polymorph was later considered in terms of the distribution of heat of crystallisation on nucleation [63]. This explanation is different to that cited by Ostwald, prior to the establishment of irreversible thermodynamics, which is based on an analogy with gas-liquid behaviour and has some inconsistencies [63]. According to Threlfall, whether a multi-step mechanism is favoured over direct formation of the stable state will be highly condition dependent and governed by the minimisation of free energy, ΔG, as well as the rate of entropy production. It is suggested that the polymorph formed will be contingent on factors such as the enthalpy of crystallisation, solution concentration and nucleation rate. According to Threlfall, therefore, despite the prevalence of this behaviour, Ostwald's rule is *not* a universal law [63].

There are several indications in the original work that imply Ostwald himself believed the rule of stages to be constant – that the lack of observation of certain less stable polymorphs in some cases was exclusively due to accelerated transformations to the more stable states [63]. If this were the case, for glycine, it would imply there was no direct route to the formation of γ-glycine. So, any process which apparently produced this polymorph would have somehow simply affected the *kinetics* of the polymorph step cycle. There is even an indication that he believed the separation of liquid phases or "oiling" to be part of the same process.

However, from experimental observations it certainly seems as though γ-glycine can be formed directly. This is consistent with Threlfall's argument that the dominant thermodynamic process will be condition dependent. In particular, dependent on "the enthalpy of crystallisation, the concentration of the solution, and the rapidity of nucleation or crystal growth". It would seem then that, where there is a sufficiently large energetic benefit to the formation of the most stable state, the system can bypass the higher entropy multi-

step route, to form this polymorph directly. It is still unclear how important each of these elements is for various cases.

A helpful distinction to make is between the *thermodynamic* and the *structural* bases of Oswald's rule. There are some examples in NPLIN of preferential formation of polymorphs where the driving force may well be structural.

It is clearly the case that the rate at which solutions can arrange themselves into respective crystalline forms will be extremely important. In this sense, it is tempting to accept that the electric field induced alignment of polarisable clusters, as proposed by Garetz and co-workers [64], facilitates quicker assembly of α- or γ- structures depending on the incident light polarisation. And yet these results have proved difficult to replicate [30] [65]. Nevertheless, analogous results through femtosecond/CW NPLIN, discussed in Section 4.2.3, have drawn less criticism, so call for further investigation.

It has also been reported that filtration suppresses the formation of γ-glycine by NPLIN [66]. This supports the suggested role of impurity particles in NPLIN and in the case of colloidal-scale solute structures it would seem like their influence is structural.

4.2.2 Nanosecond Laser Polarisation Effects

It has been suggested that beam polarisation can influence polymorphism in NPLIN, within a limited supersaturation range, for glycine [67] and similarly for L-histidine [68]. The first report of polarisation control of crystal structure was published in 2002 by Garetz and co-workers – a nanosecond pulsed 1064 nm laser was used to induce nucleation in glycine with a 'polarisation switching' effect [67]. The beam polarisation is altered simply using either a Glan-Thompson polariser or quarter-wave plate. Garetz attributes the polymorph selectivity to the relative stabilisation of liquid-like glycine cluster arrangements by different polarisation states, assuming a two-step nucleation mechanism. Within a narrow window of supersaturation (S = 1.45 – 1.54), linearly polarised light was found to produce γ-glycine, inducing the alignment of rod-like precursor clusters, and circularly polarised light to produce α-glycine, aligning disk-like glycine clusters instead, as discussed extensively in a later work by Sun and Garetz [64].

This was a remarkable finding, demonstrating an unprecedented level of control over the crystallisation process. However, these results are debated as other attempts to reproduce polarisation switching since have failed [30] [65]. Claire et al. report a slight promotion of $\gamma-$glycine of only five samples by a circular polarised beam (compared with linear polarised) and only above S = 1.56 [65]. Liu, van den Berg and Alexander's attempt

to replicate the experimental conditions of Sun and Garetz yielded no evidence of binary polarisation switching whatsoever [30]. On the other hand, reports of polymorph control by CW laser trapping crystallisation as of yet are uncontested.

4.2.3 Laser Trapping Crystallisation of Glycine

Laser trapping crystallisation of glycine in D_2O was first demonstrated in 2007 [38] by Sugiyama, Adachi and Masuhara. This report describes rapid crystal formation, exclusively successful with the CW laser focused on the air/solution interface. The authors account for this effect by the supposed reorganisation of glycine molecules in sub-critical clusters by trapping and slowed diffusion.

Using a similar set up, Sugiyama, Adachi and Masuhara carried out further experiments exploring the trapping effects on the growth of a spontaneously formed crystals [39]. They found that irradiation adjacent to a spontaneously formed crystal either enhanced or suppressed crystal growth. The authors attribute this to cluster manipulation by photon pressure and Ostwald ripening. However, they do not consider potential laser absorption of glycine clusters by overtone vibrational modes – as temperature gradients may also result in such behaviour – so these observations are not necessarily compelling evidence for the trapping of molecular aggregates.

The first investigation of polymorph control by laser trapping crystallisation looks at the effects of laser power tuning [40]. The experiments are carried out in glycine/D_2O solutions. The substitution of heavy water has become common in femtosecond and CW nucleation studies to avoid temperature elevation from sustained irradiation at or around 1064 nm, corresponding to a vibrational overtone in H_2O. However, as discussed in Section 6.2, there have been instances of substitution and direct comparison without consideration of the solubility differences between H_2O and D_2O. As solubility is well known to affect polymorph selectivity, particular attention must be given to any solubility effects before attributing polymorph bias to other sources.

In the case of the laser power tuning study by Rungsimanon and co-workers, supersaturation is addressed but the saturation values are not given directly [40]. The concentration of solutions is given as 0.3 g / g which, according to interpolation of the solubility data of Jelińska-Kazimierczuk and Szydłowski [3], would give a saturation value of $S \approx 1.5$ at room temperature, which seems reasonable. The following discussion of their results can be made in the absence of exact values since no comparison will be made to glycine in H_2O results.

Rungsimanon et al. classify their glycine crystal polymorphs by FTIR measurement, identifying spectral changes for deuterated glycine, and confirm these results by single-crystal X-ray crystallographic analysis. Their assertion that no polymorph changes occur in the three hour growth period given before measurement (despite the tendency for solution-mediated transformation from α- to γ-glycine) is well supported by a temporal FTIR measurement of a spontaneously formed glycine crystal. The FTIR spectra showed that the transformation from α to γ began only after four days, with over one week required for completion. This supports the conclusion that the α and γ forms identified in their experiments were formed directly.

The authors carried out a convincing systematic study of polymorphism against laser power. Statistical significance was ensured by repeating measurements ten times at each interval. If the crystallisation were occurring by laser trapping of clusters, it may be expected that greater trapping force would cause higher local supersaturation. With the knowledge that increasing supersaturation promotes the γ-form, the expected trend would therefore be from α-form to γ-form with increasing laser power.

The experimental results demonstrate a tendency to form α-glycine at lower powers up to 1 W, with increasing probability of obtaining γ-glycine up to 40% at 1.3 W. This is followed by a slight drop to either 20 or 30% (the graph and analysis state different values) at 1.4 W, the highest power studied. These features are explained by way of a contest between laser trapping and local temperature effects. While the laser trapping increases with laser power – contributing to an overall shift towards γ-glycine formation; localised temperature elevation due to glycine itself absorbing will have the opposite effect. According to the authors, heating is non-linearly enhanced by the aggregation of glycine molecules in the beam focus, which in turn will effectively reduce the supersaturation. The absorption is attributed to the glycine molecules directly on account of their higher absorption coefficient at 1064 nm than that of D_2O. The combination of these effects results in a Gaussian distribution for the probability of γ formation with a peak at 1.4 W. This is a really interesting illustration of the complexities involved in manipulating polymorphism, while such developments in our understanding make promising steps towards greater control.

The group have even claimed to have induced CW crystallisation in an *undersaturated* solution of glycine in D_2O [41]; where crystals reportedly form within the beam focus, due to laser trapping of clusters, and then rapidly redissolve on account of the energetic cost of forming a solid in the undersaturated region. This is a very interesting result and is a strong indication of the ability of CW laser light to harness liquid fluctuations. It is highlighted in the study that this effect occurred exclusively at the air/solution interface, thought to be on account of enhanced alignment and hindered diffusion of molecules at this interface.

No crystallisation was found to occur in the solution or at the glass/solution interface (although a "large dense liquid droplet" was apparently formed here). Additionally, it was found that the polymorph formed had a laser power dependence as before, sharply peaking for γ formation at 1.4 W. These observations give rise to many questions and further investigations are needed to explore the phenomenon – in particular with regards to the laser focal position effects.

A more recent paper from the same authors investigates at the effect of laser polarisation [34]. This study looks at both undersaturated and saturated/supersaturated solutions, but considers the results separately. Interestingly, it was found that the γ crystal form was promoted further by laser trapping crystallisation in the saturated solution ($S = 1$) compared with the supersaturated solution ($S = 1.36$), in an apparent diversion from nanosecond NPLIN behaviour. The authors suggest this effect is due to the the metastability of the supersaturated solution enabling kinetic crystallisation to the α-form spontaneously, while in the saturated solution crystallisation would only occur with sufficient radiation pressure to induce γ nucleation directly. Hence, this does not contradict the idea that increased supersaturation will promote γ formation but highlights the complexities involved in these behaviours, when distinctions between local and total saturation values can lead to very different outcomes.

This complexity only increases in the analysis of polarisation effects. The unquantifiable local saturation value as well as the competing effects of cluster trapping and temporal heating due to glycine absorption are all considered in the discussion of results. Ultimately, it is found that circularly polarised light better promotes the γ-form at lower powers and this is said to be due to its more efficient laser trapping in comparison to linear polarisation. On the other hand, in the undersaturated solutions the converse is found to be true. Yuyama et al. claim the absence of liquid-like clusters in less concentrated solutions explains this behaviour, since the laser trapping alone is responsible for their assembly [34]. Overall, their comprehensive study constitutes solid groundwork for future investigation. Yet, clearly the underlying mechanisms are far from fully understood.

4.3 Conclusion

Explanations for polymorph formation in studies of NPLIN of glycine seem to mirror opposing theories of nucleation itself. Firstly, the OKE based understanding of Garetz and co-workers is strongly supported by their own observations of polarisation switching, debated by others. The various findings of Rungsimanon and co-workers on the behaviour of CW crystallisation and polymorph selectivity are accounted for by their proposed

laser trapping mechanisms. On the other hand, the finding that filtration suppresses the formation of γ-glycine in NPLIN exclusively [66] credits suggested mechanisms based on the heating of impurity particles. All this, highlights the importance of new research in this field, where findings seem to echo conclusions arrived at in the authors' other works without necessarily connecting up. It is very possible that there are several mechanisms for NPLIN. However, it is still unclear when or why these come into play.

Chapter 5

Nucleation of Proteins

5.1 Motivating the Study of Proteins

A persistent challenge in the study of proteins is the growth of protein crystals of sufficient size and crystallinity to be used for structure determination studies [69]. Current methods for protein crystallisation are far from ideal – often time-consuming and requiring expert technique. Protein crystallographers rely heavily on experience, as optimal conditions for crystal nucleation and growth are challenging to predict. Even with the most accomplished protein crystallographer manipulating conditions to facilitate crystal growth, enabling a critical nucleus to form spontaneously takes time (typically days to weeks).

One conventional way to lower the crystal nucleation barrier is to prepare a more supersaturated solution, but in doing so the likelihood of multiple nucleation events is simultaneously increased and hence the growth of the crystals as the concentration of the solution decreases is stunted. By increasing the supersaturation, the crystallinity suffers. Too high a protein concentration can lead to the formation of an amorphous precipitate, preventing crystallisation altogether. The phase diagram of a protein solution is complex – its state and stability depends, not only on protein concentration, but also salt concentration, temperature and pH (or in the case of heavy water solutions pD*). Understanding the stability of such a solution with respect to nucleation is therefore more challenging than the KCl and glycine systems discussed previously.

For a number of years, it has been suggested that the existence of concentration fluctuations in the proximity of liquid-liquid demixing critical points may influence crystal

*The pD value for D_2O solutions can be obtained by adding 0.41 to the measured value of the pH meter [42]

nucleation [23] [70]. Recent studies have successfully induced crystallisation of proteins with laser light and in some cases have attributed this to optical trapping of liquid-like clusters [36]. In theory, if it were possible to increase the supersaturation locally by optically trapping a small phase separated droplet – promoting crystallisation at the focus – a crystal could be induced to form slowly and well at a lesser degree of bulk supersaturation. At this stage, it is still unclear whether the laser-induced protein crystallisation observed has occurred by this method; further study is needed to determine a connection. Understanding laser effects in the protein phase diagram would be hugely advantageous, not only to protein crystallographers, but also to physical scientists seeking to understand the nature of interactions between light and matter.

5.2 Lysozyme

Lysozyme (1,4-β-N-acetylmuramidase) is an antimicrobial enzyme common to many plants and animals. In humans, it is a key component of the innate immune system – found in tears, saliva, and milk. Lysozyme acts to prevent bacterial infection by hydrolysing the polysacharride bonds between amino sugars comprising peptidoglycan, a key component of bacterial cell walls. Lysozyme itself is a small and highly stable protein, made up of 129 amino acids [71].

Lysozyme is readily obtainable from hen egg white – due to its high protein content and the ease of cost-effective purification [72]. Lysozyme from hen egg-white is a representative model sample used for protein crystallization studies – since the number of nucleation sites, and hence crystals formed, scales controllably with concentration. Hen egg-white lysozyme (HEWL) is also relatively inexpensive and has been used widely in the literature upon which this study is based. HEWL is advantageous in that it remains active over a broad pH range (pH 6 – pH 9), it is most stable with respect to thermal denaturing at pH 5 [72].

5.3 The Significance of Liquid-Liquid Separation in Lysozyme Crystallisation

The effects on crystal nucleation of lysozyme with respect to a liquid-liquid phase boundary are considered in depth by Galkin and Vekilov [73]. The authors find that crystal nucleation is considerably enhanced in proximity to a liquid-liquid phase boundary, where

visible demixing of liquid phases occurs. It is highlighted that this behaviour will rely on specific conditions being met, as the liquid demixing must occur more rapidly than the crystal nucleation. While the precise manipulation of the protein phase diagram to enable this is non trivial, this paper clearly demonstrates a connection between liquid-liquid phase separation and crystal nucleation in lysozyme. The authors even consider whether liquid-liquid separation and crystal nucleation may be viewed as two parts of the same process.

In a later study by the same authors, the reliability of this result for use in promoting crystal nucleation is questioned [74]. Experiments find the nucleation rate in the region of the liquid-liquid phase boundary to be lower than predicted at that temperature and concentration; yet in direct proximity to this phase boundary nucleation rates were found to fluctuate up to a factor of two in repeated experiments. Some variation in rate is expected as nucleation is well known to be a stochastic process, however the significance of this difference fails to support their previous conclusions. The dismissal that this is due to unknown "minor shifts in experimental conditions" is frustrating in the search for understanding and challenges the assertion that greater control over the process may be achieved by the manipulation of liquid-liquid critical points.

5.4 NPLIN of Lysozyme

To date there have been a number of studies published investigating CW/femtosecond NPLIN in protein solutions, usually HEWL, some of which [35] [36] [37] were discussed previously as evidence for a laser trapping mechanism for NPLIN in Section 2.3. These early studies clearly demonstrate the occurrence of NPLIN in lysozyme and generally account for this by the purported laser trapping of liquid-like clusters in solution incurring nucleation. The descriptions of this mechanism given are vague, and so the search for a clearly demonstrable explanation continues.

Interestingly, a more recent investigation by Yoshikawa et al., examining the energy dependence of femtosecond irradiation effects in HEWL solution, identified an energetic threshold for NPLIN of lysozyme crystals [75]. This is consistent with the results discussed in Section 2.2 for NPLIN in smaller molecules and the generation of cavitation bubbles. In a clear divergence from the laser trapping mechanism, these results appear to indicate that laser-induced bubble formation may have a role in the NPLIN of proteins. The authors, including a number of those responsible for previous literature discussing the function of optical trapping of clusters, state that their updated understanding of the mechanism for femtosecond NPLIN is based on 'morphological changes'.

Yoshikawa et al. identified the laser-induced formation of vapour bubbles in HEWL by high speed imaging [75]. Some of the bubbles imaged were observed to shrink after growth while others persisted. These bubbles were attributed to the vaporisation of water, on account of the similarity in size of vapour bubbles produced from pure water. In this paper, the authors advise that multiphoton absorption at the laser focus causes thermoelastic pressure, forming a shockwave that results in a cavitation bubble. They suggest that these cavitation bubbles may induce crystal formation on their expansion and collapse by *either* mechanical agitation from pressure fluctuations *or* by local condensation of protein molecules.

Despite there being wide evidence for an association between laser-induced bubble formation and NPLIN, it seems strange that these papers do not investigate the laser-induced bubble formation itself further. The mention of multiphoton absorption is not expanded upon. Compared with the glycine and KCl solutions discussed previously, HEWL solutions contain many more components but from the literature it is not obvious what is thought to be absorbing on irradiation. Murai et al. examined the effect of laser wavelength on NPLIN efficiency, comparing 780 nm with 260 nm (where one-photon electronic absorption occurs from amino acids' aromatic rings) [76]. Laser irradiation, above the threshold energy, was found to induce crystallisation at both wavelengths.

A subsequent illustration shows the accumulation of protein molecules (slower moving than the rate of cavitation expansion) around a cavitation bubble, which then collapses, leaving behind a concentrated region where a crystal is formed [77]. Experimentally, high speed imaging carried out by Iefuji et al., using glucose isomerase as a model protein, shows a bright region left behind after the disappearance of a bubble [77]. According to the authors, this is indicative of high concentrations of cytochrome c that likely induces subsequent crystal formation – supporting their suggested mechanism based around laser cavitation induced concentration gradients. Their nucleation probability results confirm that femtosecond irradiation promotes crystal formation, even in regions where crystals are not known to form spontaneously, and the evidence for accumulation of protein molecules on bubble collapse is very interesting. However, the suggested link between the locally concentrated regions imaged and the crystals visible in solution *two-weeks* later is not sufficient to define the mechanism for NPLIN.

In conclusion, following the optical trapping approach initially suggested on observation of NPLIN of lysozyme, more recent experiments have drawn focus on cavitation bubble collapse as a potential precursor to protein crystal nucleation. While there is some evidence to support this mechanism, it is by no means conclusive. Direct observation and analysis of the sequence of events leading up to crystallisation for various protein solutions would

be necessary to corroborate this idea. In addition, most recently, laser irradiation affects on spontaneously generated HEWL crystal growth have been recorded [78] and crystallisation triggered after stopping irradiation at the glass/solution interface [79]; both of these results are interpreted by the trapping of liquid-like clusters. The incidence of both laser trapping and bubble formation/collapse in protein solutions and their relationship to crystal nucleation remains undetermined.

Chapter 6

Solubility

The solubility of a substance at a given temperature is an important value in nucleation experiments, as it dictates the degree of saturation and hence the stability of the solution. Saturation value, S, is defined as

$$S = \frac{C}{C_{\text{sat}}} \tag{6.1}$$

where C is the concentration of the solution and C_{sat} is the temperature-dependent solubility of the solute in the solvent. Solubility curves mark out the interface between stable and metastable phases. As solute concentration is increased, the solution will become increasingly supersaturated and less stable with respect to nucleation, as it is pushed further into the metastable region of the phase diagram. The height of the energetic barrier to crystal nucleation, as described by CNT, is entirely dependent on saturation [6]. As we will see, the degree of saturation of the solution also has implications for the polymorphic outcome of the crystals it forms – in substances which can produce multiple crystal polymorphs under normal conditions, such as glycine. Hence, in studying crystal nucleation from solution, it is crucial to have accurate solubility data in order to reliably calculate the saturation values.

Significant variations for the solubility of compounds in H_2O and in D_2O have been demonstrated [1] [3]. The necessary use of D_2O as solvent for the experiments described in this report (due to its reduced absorption at the laser wavelength) and corresponding lack of solubility data available, has emphasised the importance of investigating the reliability of solubility data in reporting nucleation experiments.

6.1 KCl

It is not uncommon to find some discrepancies in published solubility data, so the lack of solubility data for compounds in D_2O available for comparison must be highlighted. A table of solubility data for KCl in D_2O was published by Sunier and Baumbach [1]. These data were used as the basis for all concentration calculations in the experiments carried out on KCl outlined in this report.

Ideally, solubility measurements would also have been carried out in the lab in order to investigate the reliability of these published results. However, an indication of this can be obtained by directly comparing the results of Sunier and Baumbach for the solubility of KCl *in* H_2O (published in the same paper) with a reliable reference – where data for the solubility of simple salts in H_2O is readily available. A direct comparison of the solubility data for KCl in H_2O is shown in Figure 6.1 – with the data of Sunier and Baumbach (pink diamonds) plotted alongside that of the CRC Handbook of Chemistry and Physics [2] (green circles).

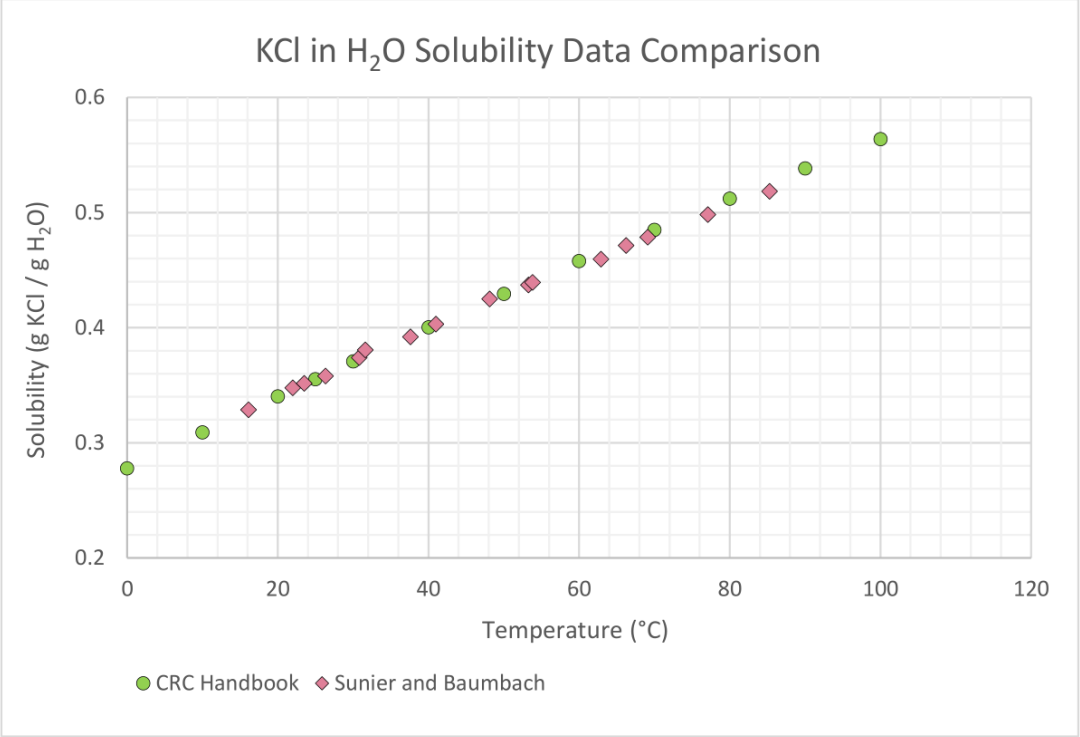

Figure 6.1: KCl in H_2O solubility data plotted against temperature. This shows consistent results between the CRC handbook data [2] (green circles) and that published by Sunier and Baumbach [1] (pink diamonds).

The CRC data was originally given as mass percent of solute, $100 \times w_2$, where

$$w_2 = \frac{m_2}{(m_1 + m_2)} \tag{6.2}$$

m_2 is the mass of KCl and m_1 is the mass of water. From this, the mass of KCl per gram of water was calculated as follows:

$$\frac{m_2}{m_1} = \frac{w_2}{(1 - w_2)} \tag{6.3}$$

Once the original data had been recalculated as solubility in g KCl / g D_2O, the values at various temperatures (in the range 0 °C – 100 °C) were plotted against the data of Sunier and Baumbach. Figure 6.1 shows consistent results in the two data sets. From this, it can be assumed that the KCl in D_2O data, published alongside the KCl in H_2O data is similarly reliable.

KCl is considerably less soluble in D_2O than in H_2O, so it is important to work with the correct numbers when calculating for experiments. More restricted atomic vibrations in D_2O result in a strengthened bonding network [80]. As it takes more energy to disrupt D-O bonds than H-O bonds, it follows that there would be a corresponding lower solubility in D_2O. Figure 6.2 shows the solubility values at various temperatures in H_2O vs that in D_2O, with an average difference of 46 mg / g in KCl. This considerable difference, although initially surprising, was consistent with our own experimental observations.

Although the data available only covers temperatures above 21 °C, a reasonable estimation of the degree of saturation was then obtained by plotting the solubility in g KCl / g D_2O against temperature, and extrapolating to lower temperatures. Experimentally, using the Linkam temperature control stage, it was much more manageable to work at lower temperatures (e.g. -5 °C) as the solutions could be made up undersaturated at room temperature and handled with ease, without the risk of inducing nucleation on transfer to the microscope stage.

Figure 6.3 shows the same solubility data, fitted with a second-order polynomial. The equation of the polynomial fit could be used for simple calculations of solubility values at lower temperatures. This in turn could be used to calculate saturation values. See below for an example of this used in experimental calculations.

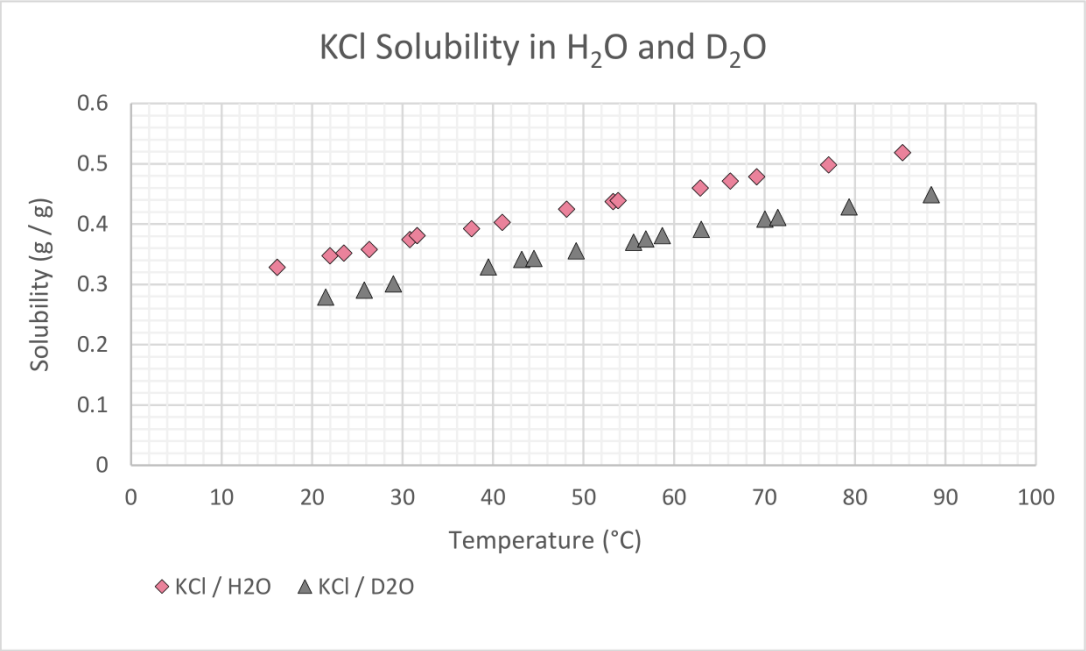

Figure 6.2: Sunier and Baumbach [1] solubility data for KCl in H_2O (pink diamonds) and KCl in D_2O (grey triangles) plotted against temperature.

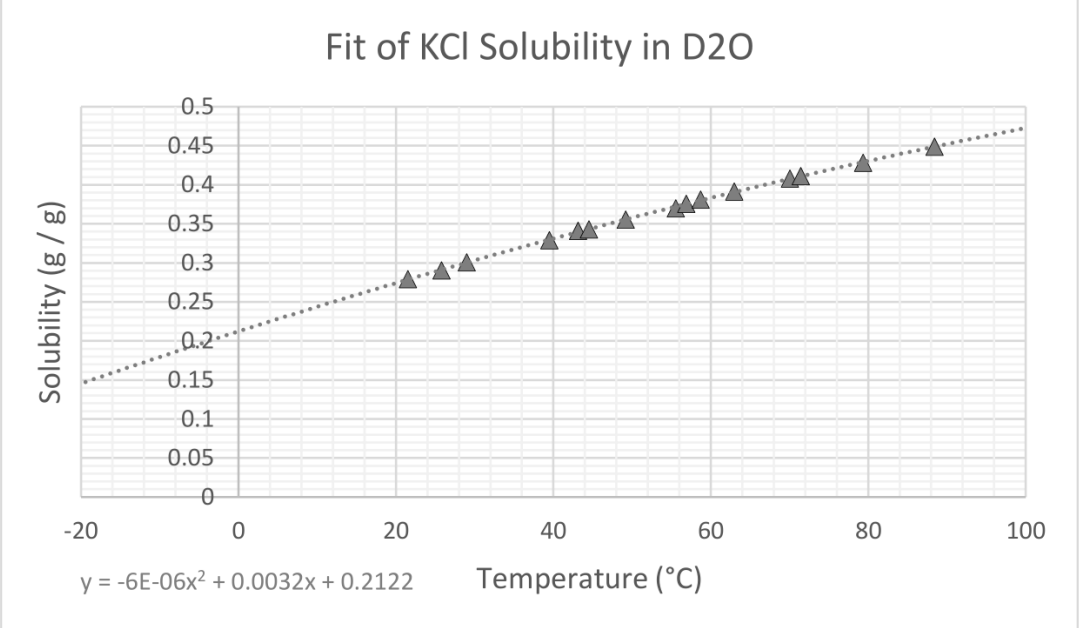

Figure 6.3: Sunier and Baumbach [1] solubility data for KCl in D_2O (grey triangles) plotted against temperature with a second-order polynomial fit showing extrapolation forecast.

6.1.1 Example Experimental Solubility Calculation

For these experiments, practical restrictions were important to consider in the calculation stage prior to making up solutions to ensure that the experiments could be carried out completely. A typical pre-experimental calculation for KCl solution is outlined below.

1. In order to avoid the samples nucleating during the experimental set up, the concentration of solute should be below saturation concentration at room temperature (the lab temperature was measured to be 21 °C).

   Using the equation of the polynomial fit to solubility data (from Figure 6.3). Replacing x with temperature, T, and y with solubility, C_{sat}.

$$C_{\text{sat}} = -6 \times 10^{-6}\, T^2 + 0.0032\, T + 0.2122 \tag{6.4}$$

$$\implies C_{\text{sat}}\,(\text{at}\, T = 21\,^{\circ}\text{C}) = 0.277\,\text{g KCl / g } D_2O$$

   This gives the solubility value at 21 °C. So if a solution is made up in the lab with 1 g D_2O, adding below 0.277 g of KCl will mean it is readily soluble and can be handled easily. For the purpose of this example calculation, say a solution is made up to give $C = 0.225$ g / g D_2O.

2. The reported saturation value required for NPLIN in picolitre droplets was $S = 1.20$ [43] and the range required for NPLIN of bulk solutions $S = 1.05$ – 1.10 [15]*. So for microlitre sized droplets, as used in these experiments, it would be reasonable to assume a saturation value $1.05 > S \leq 1.20$ was required.

   The concentration of the solution, $C = 0.225\,\text{g KCl / g } D_2O$ is independent of temperature. The solubility at $T = -5\,^{\circ}\text{C}$ can be calculated using Equation 6.4 as before, giving $C_{sat}\,(\text{at}\, T = -5\,^{\circ}\text{C}) = 0.196\,\text{g KCl / g } D_2O$.

$$S = \frac{C}{C_{\text{sat}}} = \frac{0.225}{0.196} = 1.14$$

   So the saturation value of the solution at $T = -5\,^{\circ}\text{C}$ will be $S = 1.14$. S can be varied simply, to control the stability of the solution, by changing the temperature of the stage and hence the solubility of the sample droplet, C_{sat}.

*It should be noted that these results were obtained using nanosecond pulsed lasers and so could only serve as some indication of where to look and cannot be directly compared without considering the nucleation may be occurring by a different mechanism.

6.1.2 Future Experimental Work

In theory, in terms of the sample droplet, only its saturation value should dictate the likelihood of successfully inducing nucleation. However, given more time in the lab, it would have been interesting to look exactly at the effect of temperature/laser heating.

This could be investigated systematically by making up a series of solutions of different concentrations, so as the saturation value could be kept constant while carrying out experiments at different temperatures. Holding other variables constant (such as the laser power) to obtain a set of data could give some indication of the role of laser heating in femtosecond laser-induced nucleation. Since according to CNT only S is important, any effect of varying temperature specifically could provide more information to illuminate the underlying mechanisms. It has previously been observed for nanosecond-pulsed NPLIN in KCl that the lability of samples of equal supersaturation at different temperatures diverged [46]. This study was limited to two solution temperatures, 10 °C apart, but showed greater likelihood for nucleation at the higher temperature. It would be interesting to investigate whether this effect was the same for femtosecond NPLIN.

6.2 Glycine

Reduced solubility in D_2O is not invariably the case for all amino acids, as shown by Jelińska-Kazimierczuk and Szydłowski in their paper comparing solubility of various amino acids in water and heavy water [3]. While for glycine (mixture of α and γ polymorphs), as for KCl, solubility in D_2O is lower than that in H_2O; proline on the other hand shows the exact opposite trend; while the relative solubility of phenylalanine in D_2O and H_2O is found to vary with temperature. This is surprising, and emphasises the complexity of the actual molecular interactions that underlie the concept of solubility.

The effect of deuteration on polymorphic outcome in the crystallisation of glycine is considered in a 2009 paper by Hughes and Harris [59]. In this report, the authors explore the isotope effect on polymorph selectivity, based on an observation made in 1961 by Iitaka that γ crystals formed more frequently from heavy water solutions [61]. Despite the γ-form being the most thermodynamically stable polymorph, the α-form is more commonly formed from aqueous solution under ambient conditions – the kinetically controlled outcome [34]. Hughes and Harris suggest that the percentage deuteration of a glycine solution directly affects the polymorphic outcome. However, they completely disregard solubility considerations. Given the differences in solubility values for H_2O and D_2O, varying the

percentage deuteration of a glycine solution will clearly impact the solubility of glycine in that solution. So it is misleading to claim that the percentage of deuteration will affect the polymorphic outcome directly without further investigation of the solubility changes it brings about.

In fact, it has since been shown that the polymorphic outcome of glycine crystallisation *is* supersaturation dependent [30]. It has been demonstrated, using various methods of inducing nucleation (sonocrystallisation, mechanical shock and NPLIN), that increasing the supersaturation of a glycine solution made it in all cases more likely to form γ-glycine crystals after nucleation, as opposed to α-glycine. This is actually consistent with the observations made by Hughes and Harris [59].

Hughes and Harris found that higher percentage deuteration – which for glycine implies decreasing the solubility and (according to Equation 6.1) therefore increasing the supersaturation – tended to promote the formation of the γ-form. They explain this in terms of an increased rate of transformation from α to the more stable γ in the presence of deuterium, but suggest other work is necessary to explain the underlying mechanism.

Although Alexander discusses the results in terms of the cavitation mechanism for nucleation, and thereby accounts for differences between results for mechanical shock, sonocrystallisation and NPLIN. No further explanation of why high supersaturation should favour γ-glycine follows. As discussed in Section 6.2, there may be thermodynamic or structural bases for polymorphic inclination. At higher supersaturations, diffusivity is considerably reduced [81]. It could be that the underlying solution structure at higher concentrations makes a helical 3D network γ-type arrangement more accessible. In addition, the degree of supersaturation is known to affect the height of the energy barrier to nucleation, so it is likely that a thermodynamic explanation exists.

According to Ostwald's rule the crystal phase formed will most likely be that closest to the liquid in free energy, which is commonly α in the case of glycine. Changing (increasing) the free energy of the solution by increasing supersaturation would imply the preference may shift.

6.2.1 Future Experimental Work

It would be interesting to further investigate the purported link between deuteration and polymorphic outcome. While the disregard for solubility differences in Hughes' study casts doubt on their conclusion; it has elsewhere been claimed that a transformation from α- to γ-glycine, in powder form, occurred more readily for the deuterated sample [61]. Again,

this description lacks a detailed account or explanation of such a result. It is entirely possible that this observation is just one of the many random polymorph behaviours found to occur (see Section 4.1) and unconnected with the percentage deuteration. However, it is interesting that this behaviour has been widely accepted and referenced without much experimental analysis. If there were some tangible effect on crystallisation by replacing water with heavy water as a solvent – accounting for known solubility differences – this would be very surprising.

In terms of NPLIN, polymorph control by polarisation switching in femtosecond/CW laser irradiation also warrants further study. While this effect is debated for nanosecond NPLIN, results for femtosecond/CW are apparently less controversial. It would be useful to replicate the polarisation switching results and to investigate such a correlation further in order to better understand the mechanism at play. To confirm a link between polarisation and polymorph formation in glycine by femtosecond laser NPLIN would provide strong evidence for the trapping and orientation of molecules in the beam. Such a demonstration has potential to bring about an unprecedented level of control over crystallisation.

Chapter 7

Other Considerations

7.1 Dust and Impurities

The avoidance of excessive dust particles in samples, which may provide heterogeneous nucleation sites, is important in any attempt to study homogeneous nucleation. As discussed in Section 2.2.1, it has been widely observed that nano-filtration suppresses NPLIN in various solutions. It has been found that the presence of impurity particles, in particular, may significantly impact crystallisation results [16]. For these reasons, the use of purified chemicals, clean glassware, and minimum exposure of solutions and containers to air was ensured for our own experiments. The solutions were customarily filtered using $0.2\,\mu$m pore size filters, unless otherwise stated for the investigation of filtration effects.

7.2 Sample Ageing

Many nucleation studies have discussed the *ageing* of supersaturated solutions and related effects on the likelihood of crystallisation. Since nucleation of metastable solutions may occur spontaneously, leaving vials of solutions, to be tested for NPLIN, untouched for several days before experiment enables clear identification of the fraction of samples spontaneously nucleated and chance to remove those before irradiating the others. It is not immediately obvious though how ageing may otherwise effect the solutions.

Zaccaro et al. go so far as to claim that ageing of solutions is a "necessary prerequisite" for nucleation [19]. From our own observations this is simply not the case – solutions can be irradiated immediately and produce crystals, at least in KCl. However, the age

of solutions is something that has been discussed extensively in nucleation studies and various compounds reported to respond differently, so it is worth some consideration.

Unfortunately, these reports often offer little explanation themselves as to why ageing may effect the lability of solutions, and considering the timescales of liquid dynamics it is unclear why ageing of days to weeks would alter the composition significantly at moderate concentrations in a sealed container. Zaccaro et al. indicate that the ageing may facilitate cluster formation – or the first step in the proposed two-step mechanism (as discussed in Section 2.1) [19]. In their report on laser-induced crystallisation of glycine, the authors state that non-aged samples did not nucleate with laser irradiation, whereas samples that had been aged for four days prior did. For such a surprising statement, no further information is given on the fraction of samples nucleating in each case, or the significance of the timescales used.

One paper which provides a more detailed account of ageing effects in metastable glycine in terms of time-dependent diffusion coefficients is cited by Zaccaro et al. [81]. Myerson and co-workers have employed Gouy interferometry to look at diffusivity in various solutions including urea [82], KCl [49] and glycine [81] solutions. Their experimental results show – for supersaturated solutions – a sharp decrease in the diffusion coefficient with increasing concentration. It is suggested that this may be due to the formation of clusters in supersaturated solutions with increasing concentration, with diffusivity dropping to zero at spinodal. Interestingly, the authors justify a similar result for KCl solutions. It is unclear exactly what is meant by a drop in diffusion coefficient due to cluster formation in KCl, with no solute molecules present to cluster.

The effects of ageing are examined directly by Myerson and co-workers for glycine and lysozyme solutions only. Myerson and Lo find that aging of glycine (from 1 hour to ≈ 100 hours) corresponds to a reduction in diffusion coefficient value, at various supersaturations [81]. They attribute these results to the 'evolution' of pre-existing clusters in the solution, suggesting that clusters continue to grow slowly, following their rapid formation. From this paper alone, it remains unclear why ageing of several days would be necessary for NPLIN. This does little to support the case for a two-step mechanism for NPLIN based on diffusion-controlled cluster formation because the significance of ageing or slowly growing clusters in the facilitation of laser-induced crystal formation is not explained.

Interestingly, Kim and Myerson find that the ageing of lysozyme solutions has no such impact on the diffusion coefficient, though varying salt concentration does [83]. In an investigation of NPLIN of HEWL solutions by Lee et al., it is stated that laser-induced crystallisation is more effective with shorter ageing time [37] (by contrast to the much longer glycine studies, ageing times of 10 minutes to 3 hours were considered). The

authors claim this effect is likely due to high concentration fluctuations after mixing and the presence of liquid-like clusters, which become smaller and fewer as the solution becomes well mixed. This observation could also be deemed consistent with a two-step nucleation mechanism, however the nature of the supposed first step clearly differs considerably from the slow growth of glycine clusters described.

A thorough experimental investigation of these effects would be helpful as contrasting views on the importance of ageing persist. For salt solutions, like KCl, aging does not seem to affect the incidence of NPLIN at all. In terms of NPLIN studies of glycine, often different ageing times are given without further explanation. If ageing effects were clearly demonstrated, their cause and relation to proposed two-step mechanisms for specific compounds would require further attention. Within the literature on NPLIN, ageing effects are too often cited without further explanation. Current evidence is inconsistent and therefore does not provide substantial support for any particular nucleation mechanism.

Chapter 8

Methodology

8.1 General Experimental Design

An outline of the main experimental set-up used in this investigation is shown in Figure 8.1. For imaging phase changes in small ($\approx 20\,\mu$l) droplets, an Olympus BX53 upright microscope was fitted with Olympus UPLFLN 10× and LUCPLFLN 20× objective lenses and connected up to an Andor Zyla sCMOS camera, enabling image capture.

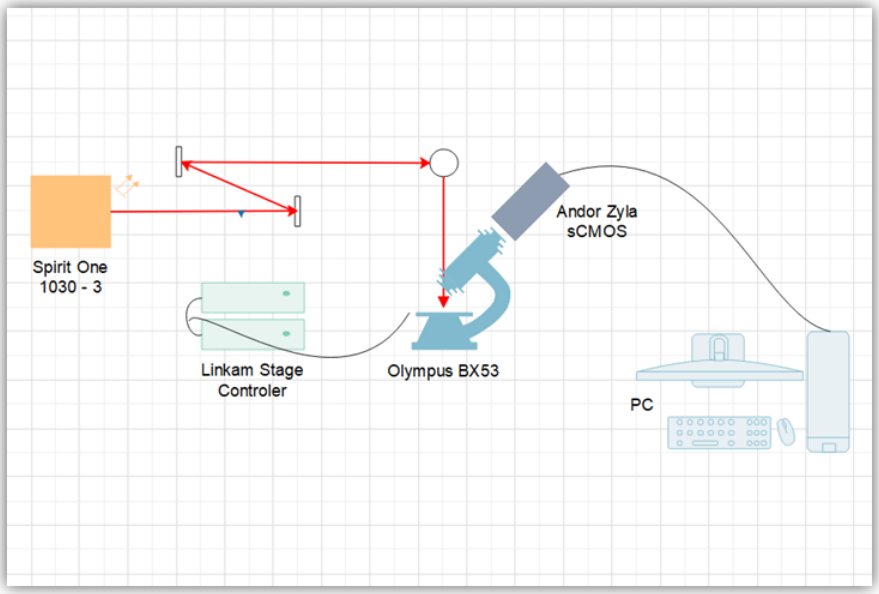

Figure 8.1: Diagram showing main components of experimental lab set-up.

The sample droplets were held in a sealed Linkam TMS600 stage (Figure 8.2) connected

to a Linkam LNP96 cooling system, allowing for complete temperature control during the experiments, with a quoted 0.01 °C accuracy.

The laser used to irradiate the samples was a SPIRIT ONE 1030-8 femtosecond pulsed laser. The laser beam was aligned through the microscope objective to fall on the sample by a series of optics. The laser was set to 1 MHz repetition rate with a pulse duration of 4000 fs. The power could be altered within the range $0-9$ W. The highest power reached in our experiments was 2 W. The power could be measured at various positions in the optical set up using a Coherent FieldMaxII-TO power meter.

All samples were initially prepared as ≈ 1 ml volumes in 4 ml clear glass screw neck vials. The solute concentrations were calculated by mass, and components measured out using a Sartorius CP64 analytical balance, to allow for accurate calculation of final concentrations. All concentrations are, therefore, given as mass solute per gram D_2O (g X / g D_2O).

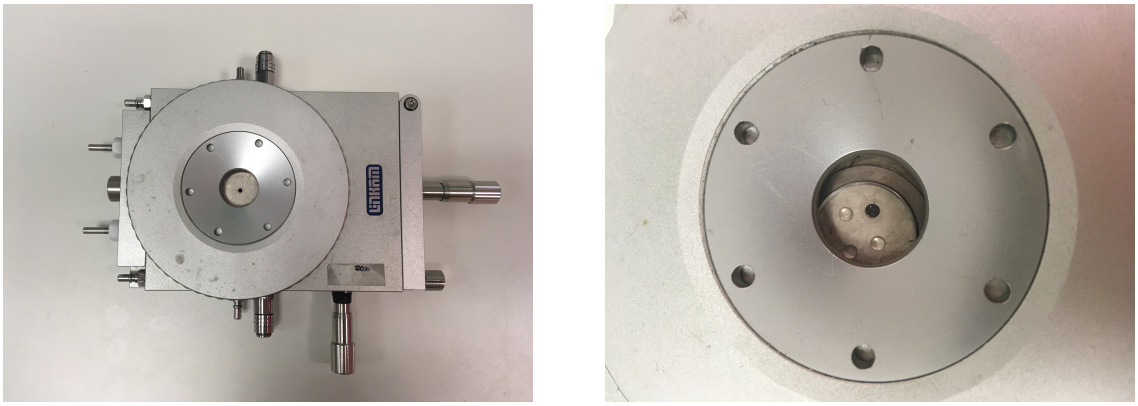

(a) **(b)**

Figure 8.2: Linkam TMS600 temperature controlled microscope stage: (a) shows manual xy translation controls and (b) sealed stage containing four sample droplets, one positioned over central illumination cavity.

The Linkam stage containing the sample was centred and attached to the microscope so that the central channel would allow for illumination through the underside. The Linkam TMS600 was connected up to the LNP96 controller and liquid nitrogen dewer. The temperature was controlled via the PC using LinkSys32 software, or the external controller.

8.2 Set-Up

Once the required mass of solute was calculated (see Section 6.1.1 for example calculation), this was measured out using the balance directly into the 4 ml screw neck vial along with $\approx$ 1 g of D_2O, ensuring the exact masses were recorded. The solid was then dissolved, depending on concentration either by careful swirling of the vial (to avoid bubbles) or, if necessary, the vial could be heated in the oven to dissolve the sample. For the most part, carrying out experiments at temperatures below 0 °C meant the solid was readily soluble at room temperature. Once the solute had fully dissolved, the solutions were filtered using Millex-LG (SLLG025SS) 0.2 μm pore size, hydrophilic PTFP membrane syringe filters into clean 4 ml screw neck vials.

For each experiment, a new 16 mm diameter VWR 100 pcs borosilicate glass slide (Figure 8.3 (a)) was placed carefully inside the Linkam TMS600 stage. When working at room temperature, a spacer followed by a borosilicate cover glass was placed over the sample so as to slow evaporation. For a non-invasive separator Thermo Fisher Scientific, Invitrogen, Secure-Seal^{TM}, 0.12 mm deep spacers were used. Rectangles containing eight 9 mm diameter wells, were easily cut into separate circular spacers of the appropriate size, as shown in Figure 8.3 (b). One circular spacer was adhered to the glass slide in the Linkam stage. One or more $\approx$ 23 μl droplets of the sample solution were pipetted from the 4 ml vial onto the glass slide, well within the walls of the spacer, and the sample quickly covered.

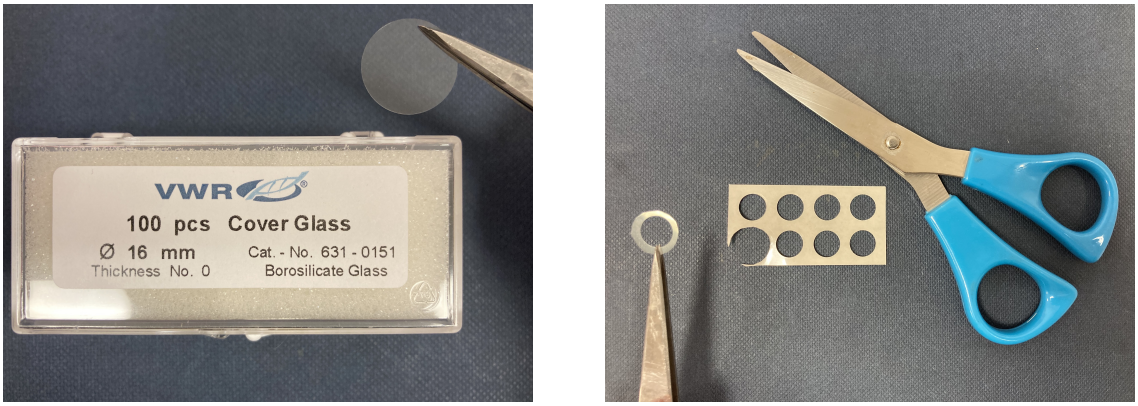

(a) **(b)**

Figure 8.3: Some key components of the experimental set-up: (a) VWR 16 mm diameter glass slides and (b) Thermo Fisher 0.12 mm depth spacers.

Using the Linkam built-in xy translation, the droplet was moved to be just covering the central hole in the base of the stage. The Linkam TMS600 stage was then connected up to the temperature control system and the sample ready to test.

Chapter 9

Experimental Results and Discussion

9.1 Use of D_2O as Solvent

From the previous literature study, it was noted that D_2O was, in some cases, used in place of H_2O as the solvent for glycine [41] [84] and lysozyme [42] solutions being nucleated by NIR CW or femtosecond lasers. From comparison of NIR spectra, it is evident that heavy water absorption is much lower than that of water at and around 1030 nm (the laser wavelength used in these experiments) [85] [86]. The absorption peak in H_2O at 970 nm is an overtone band of an O-H vibration. This band is shifted to a much longer wavelength for D_2O, making it a more suitable solvent for use in femtosecond NPLIN experiments at 1030 nm.

Initially, solutions of glycine and lysozyme were made up using H_2O. Irradiation of H_2O solutions at laser powers of up to 1 W lead to violent boiling and the rapid formation of bubbles at room temperature, confirming the IR absorption. This was clearly problematic for the intended studies as intense localised heating would impact saturation value and could inhibit crystal nucleation. Therefore, D_2O was used as a solvent replacement for all subsequent experiments*.

*For lysozyme tests, the buffer solutions were prepared using D_2O without using deuterised acetic acid/sodium acetate, since the concentration of hydrogen with respect to deuterium ions in the resulting solution was negligible (the primarily D_2O containing samples did not immediately boil on irradiation at room temperature as the H_2O).

9.2 Lysozyme and Glycine Experiments

9.2.1 Lysozyme

Preliminary experiments attempting to replicate the laser-induced crystallisation effects observed by Tsuboi [36], Yuyama [79] and coworkers in lysozyme solutions were unsuccessful, with HEWL solutions made up as in Table 9.1 (see Appendix A for acetate buffer details). No obvious effect of laser irradiation was observed during these preliminary tests.

Unfortunately, lab time was severely restricted by the lockdown imposed in response to the Coronavirus (COVID-19) pandemic. Had time allowed, a systematic study varying factors such as laser power, temperature and composition would ideally have been carried out, in order to study the phenomenon more thoroughly. NPLIN in HEWL by femtosecond and CW laser irradiation has been extensively demonstrated in the literature. The process of optimising conditions to facilitate the occurrence of NPLIN may also serve to further elucidate its mechanism. The details of the solutions are included here in the hope that they may be useful as a starting point for future work on this.

For our own investigations, the HEWL concentration was set at $\approx$ 50 mg ml^{-1} to allow for quick reference to be made to the lysozyme concentration against temperature phase diagrams of Muschol and Rosenberger [70]. This would be considered a very high concentration by protein crystallographers, who use lower concentrations (typically 4 to 20 mg ml^{-1}) to grow higher quality crystals [69]. However, a high protein concentration was deemed appropriate for the purposes of identifying immediate results of any potential laser-induced crystallisation; over obtaining very well formed crystals initially.

HEWL solutions: 50 mg ml^{-1} HEWL, 0.1 M acetate buffer at pH = 4.5		
	3% (w/v) NaCl	5% (w/v) NaCl
HEWL	0.05 g	0.05 g
NaCl	0.03 g	0.05 g
NaAc	0.0287 g	0.0287 g
Ac acid	37 μ l	37 μ l
D_2O	963 μ l	963 μ l

Table 9.1: HEWL solution components

9.2.2 Glycine

The experimental testing of the NPLIN of glycine, using the set-up outlined in Section 8.2, was primarily hindered by the spontaneous crystallisation of samples. This is illustrated by the extrapolation of the glycine in D_2O solubility data, as shown in Figure 9.1. Unlike that of KCl, the glycine solubility curve begins to level off below room temperature. In practice, this meant that in order to achieve sufficient supersaturation for NPLIN effects to be observed according to previous experiments, the solution was unstable with handling at room temperature.

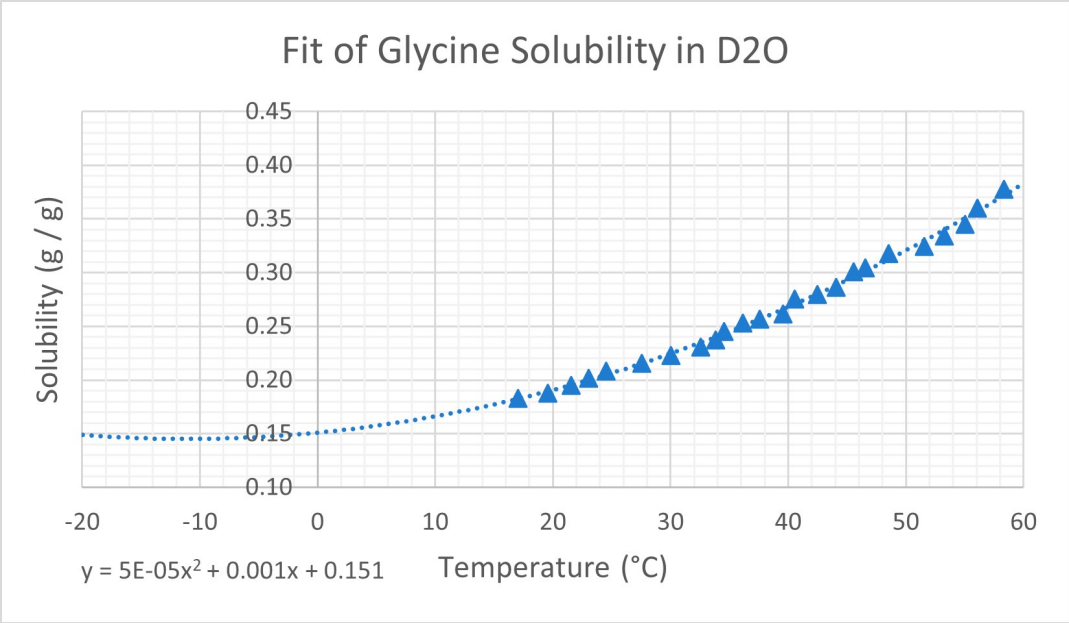

Figure 9.1: Jelińska-Kazimierczuk and Szydłowski's [3] solubility data for glycine in D_2O (blue triangles) plotted against temperature with a second-order polynomial fit showing extrapolation forecast.

For the glycine in D_2O solution preparation, in order to reach $S = 1.60$ at 25 °C, a 0.33 g / g solution must be heated to above 50 °C to dissolve the solute, and then slowly cooled to room temperature for testing. By contrast, the KCl solubility curve is steeper in this region – meaning that solutions could be made up to be undersaturated at room temperature (so that handling posed no risk of inducing spontaneous crystallisation) and would become saturated and supersaturated on cooling just below room temperature.

Various attempts were made to avoid the spontaneous crystallisation of glycine solutions such as: extended cooling periods, changing the material of the pipette tip, warming the pipette tip and slide, and quickly covering the sample to avoid evaporation. However, the unavoidable turbulence on transfer of the droplet from the vial to the slide, paired with

the gradual evaporation of solvent at room temperature inevitably encouraged nucleation before the laser effects could be investigated.

In the glycine crystallisation experiments of Sugiyama, Adachi and Masuhara [38] [39], the authors suggest that spontaneous crystallisation only occurred after ≈ 30 minutes in a 40 μl droplet, by slowly increasing saturation due to evaporation. From our own observations droplets of glycine even at low supersaturation were much more volatile and spontaneous crystallisation was rapid.

The reports do state that the glass slide on which the droplet was held was immediately sealed to suppress the solvent evaporation, and in a later set-up a sealed bottle was used [41]. Our own set-up was limited in restricting evaporation, as the spacers used could only adhere to a single glass slide. Perhaps a tailored technique and set-up could allow for more time for experiments to be carried out. It would be valuable to compare experimental set-ups directly, for the literature studies and our own, in order to account for the apparent divergence in stability of glycine solutions with respect to spontaneous nucleation. It may also be interesting to look at the effects of filtration and impurities, which may effect stability. Such an investigation to optimise conditions would require dedicated time, but given the interest in glycine as a system for NPLIN the results would no doubt prove valuable.

9.3 KCl Experiments

9.3.1 Inducing Crystallisation

Horizontal Stage Translation

Initial attempts to induce nucleation directly in supersaturated KCl/D_2O by femtosecond laser irradiation were unsuccessful. Subsequently, it was observed that crystallisation *could be induced* using the built in manual xy translation on the Linkam stage combined with laser irradiation, so as to translate the position of the laser beam focused on the sample droplet. Crystals growing outwardly from the laser spot were observed. Figure 9.2 shows the first crystal produced by this method.

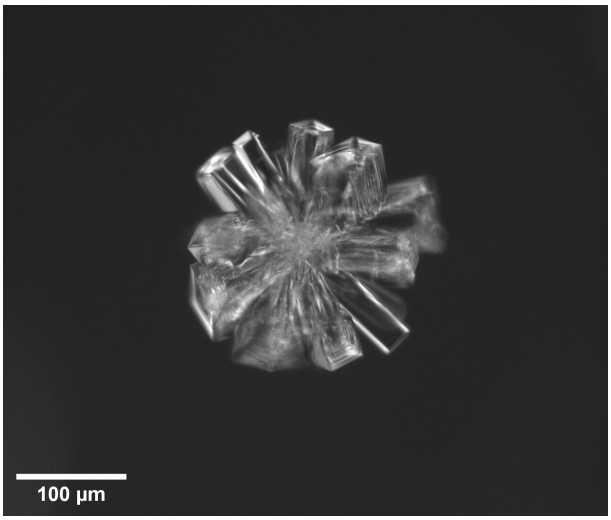

Figure 9.2: First KCl crystal in supersaturated D_2O solution produced by femtosecond laser irradiation (1030 nm) combined with xy microscope stage translation.

The radial-columnar shaped crystal, as shown in Figure 9.2 and in Figure 9.4 (a) is particularly interesting. It shows the crystal growth originating from the point of the laser focus. This contrasts with the spontaneously formed cubic KCl crystals shown in Figure 9.3, where multiple nucleation points have lead to the growth of many small cubic crystals. This clear divergence in crystal shape for spontaneous vs NPLIN was interesting but inconsistent. Evidence of cubic shaped laser generated crystals can be seen in 9.4 (b). Despite this, the crystal shape can in some cases be a helpful indicator as to the origin and evolution of the crystal growth, in what is a rapid and nanoscale process.

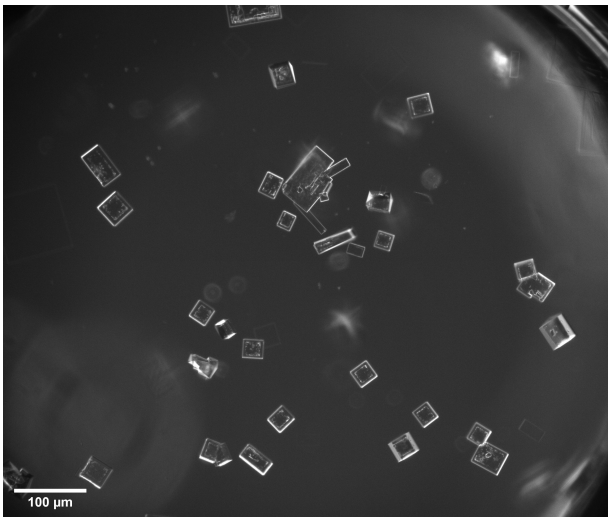

Figure 9.3: KCl crystals formed spontaneously from solution on transfer of the sample droplet to the microscope slide.

Continuing investigations found the incidence of crystal generation to be very sporadic; sometimes KCl crystals were generated rapidly and other times up to a minute of irradiation, combined with horizontal translation, was necessary to achieve nucleation. Occasionally, crystallisation would not occur at all, even under identical conditions. Despite this inconsistency, over a series of experiments, the formation of KCl crystals with laser irradiation was extensively demonstrated.

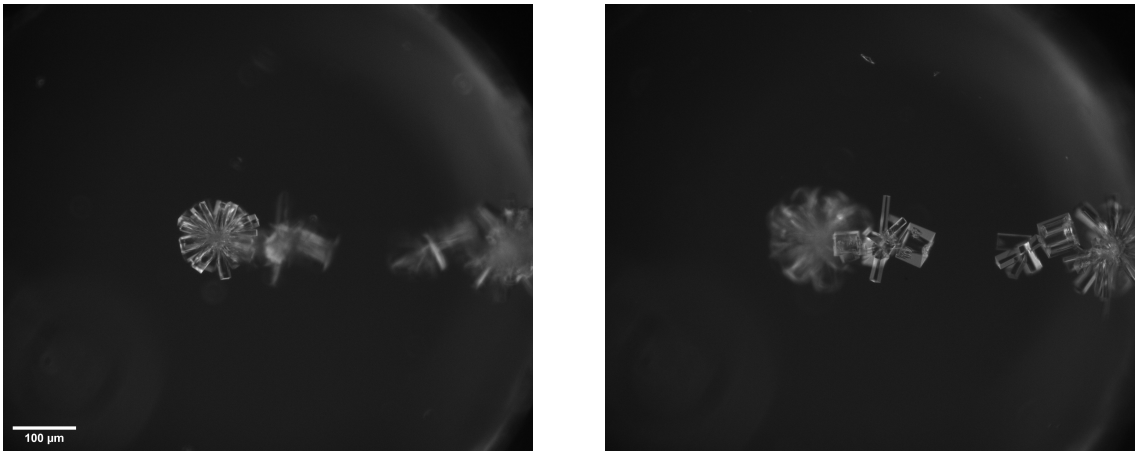

(a) **(b)**

Figure 9.4: Laser-induced crystals of KCl in D_2O with horizontal translation, showing a series of crystals growing along the laser path.

Great care was taken to avoid turbulence when translating the stage. Mechanical shock is

well known to encourage nucleation. Yet, in this case, the samples used were sufficiently stable that translation of the stage alone was never found to prompt nucleation. On the other hand, translation of the stage paired with laser irradiation was observed to repeatedly induce nucleation at the laser focus. So the KCl crystal formation observed was evidently occurring by some form of NPLIN.

Vertical Focusing

The nature of the impact of laser focus translation through the sample droplet was investigated further. It was found that changing the microscope (and therefore laser) focus in the sample could also induce nucleation, where continuous irradiation at a fixed focal position in the droplet usually would not. This gave rise to the question of whether the success of NPLIN with horizontal translation and vertical focusing was associated with irradiation at a specific focus position/depth in the sample or whether the act of *translation* of the focus position somehow aided crystallisation.

Previous studies have highlighted the importance of focal position for inducing crystallisation. Rungsimanon et al. observed NPLIN in glycine/D_2O solution by a CW NIR laser aimed exclusively at the air/solution interface [41]; whereas Yuyama et al. triggered crystallisation of lysozyme by CW NIR irradiation at the glass/solution interface [79]. The experimental set-up utilised in these experiments allowed for identification of the glass slide surface by visible dust or markings on the glass. The laser focus could then be translated upwards from that point into the droplet. From our own observations, it did not appear as though the nucleation was triggered at a specific interface but rather occurred at an arbitrary position within the droplet. As previously stated, it was apparent that the NPLIN originated at the laser focus; yet the position in the sample where this occurred was inconsistent. Further study, measuring the likelihood for NPLIN at various depths in the droplets, would be necessary to entirely dismiss significance of the focal position. However, the results of this basic study indicate that the crystallisation did not occur exclusively at particular depth or interface.

9.3.2 Bubbles

After some time it was noted that vapour bubbles were, in some instances, apparently being formed in the laser focus (see Figure 9.5). This was initially surprising as D_2O was used in place of H_2O on account of its reduced absorption at 1030 nm. On top of this, the dissolved KCl would be expected to further *reduce* absorption due to molecular vibrations

by displacing D_2O molecules in solution.

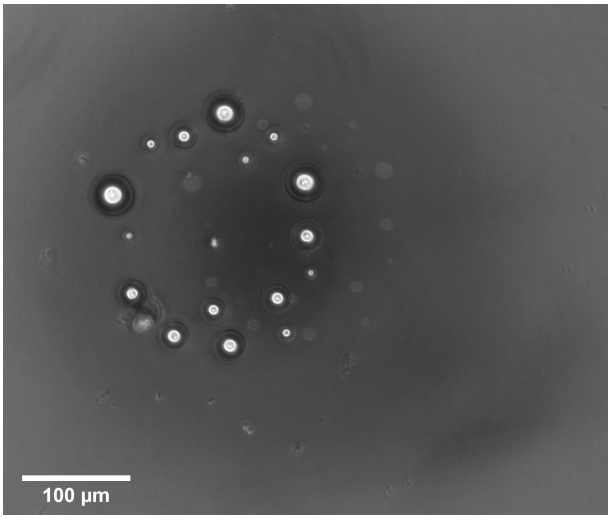

Figure 9.5: Bubbles in KCl/D_2O solution formed by laser irradiation.

It has previously been reported that laser heating has minimal effect on crystal growth rate, and additionally stated that the temperature elevation of a glass substrate is negligible [42] – though these experiments focused specifically on the effect on a growing crystal. During our investigations it was observed that KCl/D_2O solutions could consistently produce bubbles, even at low temperatures such as -10 °C. A thorough investigation was carried out in an attempt to find the cause.

Initially, it was suspected that the glass slide may have been absorbing heat from the intense laser beam. In an attempt to identify the location of the bubble production (e.g. glass/solution interface, bulk solution or solution/air interface) the solution was observed while the laser focus was vertically translated through the droplet. The laser was clearly focused on the bottom glass slide (easily identified by marks and the appearance of a reflection spot) and then the sample translated in the z plane so as to bring the focal position upwards into the solution. After repeated observations, and while the vertical focus position corresponding to the appearance of bubbles seemed somewhat arbitrary, it was clear that the laser-induced bubble formation was not occurring exclusively at the glass surface. By visual inspection, it seemed that something in the solution itself was absorbing. These observations, combined with the previous use of the same glass slides in the lab without any absorption effects, seemed to indicate that the slides were not responsible.

The possible contamination of KCl was discounted, as solutions made up from a newly purchased bottle of 99.999% pure KCl were also found to form bubbles on irradiation. An

alternative sealed source of D_2O did not appear to suppress the effect either.

It was also suggested that dust or impurity particles, possibly originating from the surface of the glass slide, may be responsible for the absorption, as in the nanoparticle heating mechanism. The necessary irradiation of a specific impurity particle, which may be as likely to be found stuck to the glass/solution as in the solution, could also account for the apparent variation in the laser focus position where NPLIN could be induced within the sample. It would also explain why, in some cases, NPLIN could be induced immediately (where such an impurity happened to be in proximity to the initial laser focus position) and in other cases would require extensive translation through the droplet or not occur at all (if the laser focus happened not to encounter such an impurity particle).

Seeking to identify the significance of dust or impurity particles, comparison was made between unfiltered and 'pure' solutions. For the 'pure' solutions: the solutions were filtered using Millex-LG (SLLG025SS) 0.2 μm pore size, hydrophilic PTFP membrane syringe filters, all glassware used was cleaned and dried thoroughly, glass slides were cleaned and dried using a 60:40 acetone methanol mix and lens tissue, gloves were worn at all times during preparation and extra care was taken to seal the solution inside containers to avoid exposure to dust particles in the lab. On the contrary, unfiltered solutions were transferred directly to new glass slides which has not been cleaned. Surprisingly, no significant difference in the incidence of NPLIN was found between the unfiltered and 'pure' solutions. Of course, the mitigation of tiny dust and impurity particles is restricted in regular lab conditions so these experiments are difficult to do well in practice. It would be interesting to investigate, as in the study of Ward, Mackenzie and Alexander with ammonium chloride solutions [16], whether intentional doping of impurity particles would increase NPLIN efficiency.

Ultimately, the attempt to identify an explanation for the absorption mechanism leading to the formation of vapour bubbles in KCl/D_2O was inconclusive. Interestingly, however, during this process it was observed that the bubble production, despite initially seeming random, did have some laser power dependence. The existence of a power threshold for bubble formation is consistent with previous observations of laser-induced bubble formation as discussed in Section 2.2.

9.3.3 Laser Power Dependence of Irradiation Effects

Measuring Power Values

It was suspected that a significant amount of the beam power may be lost on transmission through the laser-aligning optical components of the set-up, so that the power reaching the sample would be somewhat reduced in comparison with the actual output reading. The experimental set-up was not conducive to the accurate calculation of power densities at the sample, due to restricted space limiting the possible positions for the power meter. However, the power meter could be used to measure the laser power just before the objective lens, so it would be expected that the true power reaching the sample be just slightly below this.

From a measurement of five power intervals, it was found that the reading shown on the SPIRIT ONE 1030-8 display corresponded well to the power reading recorded at the laser output by the Coreherent FieldMaxII-TO power meter. The power reading pre-objective was then an average of 57.6 % of the actual laser output value. The corresponding values are shown in Table 9.2. Had more lab time been afforded, an accurate investigation of power changes would have been valuable for better quantification of the NPLIN results. A limited relative comparison can be made here using the percentage capacity values.

Laser Display Power (% capacity)	Laser Display Power (W)	Meter Recorded Laser Output Power (W)	Meter Recorded Pre-objective Power (W)
10	0.77	0.77	0.46
15	1.147	1.142	0.65
20	1.517	1.514	0.862
25	1.896	1.894	1.076
30	2.267	2.268	1.309

Table 9.2: Laser power results: comparing the SPIRIT ONE 1030-8 display readings with the power meter readings recorded at the laser output and closer to the sample (pre-objective lens).

Power vs Temperature Results

The results of a systematic study of the outcome of laser irradiation as a function of laser power and temperature (with corresponding saturation value, S) are shown in Table 9.3. The laser powers are given as a percentage value of the laser capacity as described, with

the equivalent values in Watts presented in Table 9.2. The outcome of laser irradiation and vertical focusing is indicated by letter: X = nothing visible, B = bubble, C = crystal.

T (°C)	S	Power				
		10%	15%	20%	25%	30%
20	0.69	X X X	X X X	X X X	B X X	X X X
15	0.73	X X X	X X X	X X X	B B X	B B X
10	0.78	X X X	C C X	X X C	B X B	B B B
5	0.83	X X X	C X X	X X X	B X B	B B B
0	0.9	X C X	X X X	X X X	B B B	B B B
-5	0.97	X X X	X X X	C X X	B X X	B B X
-10	1.06	X X X	C X X	X X C	C BC X	B X X

Table 9.3: Outcome of laser irradiation with vertical focusing in *filtered* (C = 0.190 g / g) KCl/D_2O solution indicated by colour and letter: (black) X = nothing visible, (red) B = bubble, (green) C = crystal. The saturation value, S, calculated from extrapolated solubility data of Sunier and Baumbach [1] is given alongside the corresponding temperature.

Filtration Effects

In an attempt to investigate filtration effects more systematically, the results of laser irradiation as a function of temperature and laser power were also recorded for an unfiltered KCl/D_2O solution (made up to similar concentration) and are presented in Table 9.4.

Comparing the outcomes presented in Tables 9.3 and 9.4, the results are unexpected. The reduced incidence of NPLIN generating a C result in the unfiltered case (Table 9.4) confirms there was no obvious suppression of NPLIN by filtration. This is surprising, as it has been widely recorded in previous studies that filtration will suppress NPLIN, with

T(°C)	S	Power				
		10%	15%	20%	25%	30%
20	0.69	X X X	X X X	X X X	X B X	X B B
15	0.73	X X X	X X X	X X X	C B X	B B X
10	0.78	X X X	X X X	X X X	X X B	B B B
5	0.83	X X X	X X X	X X X	X X X	B B B
0	0.9	X X X	X X X	X X X	X X X	B B BC
-5	0.96	X X X	X X X	X X X	X X X	B B B
-10	1.05	X X X	X X X	X C X	C X X	B X X

Table 9.4: Outcome of laser irradiation with vertical focusing in *unfiltered* (C = 0.188 g / g) KCl/D_2O solution indicated by colour and letter: (black) X = nothing visible, (red) B = bubble, (green) C = crystal. The saturation value, S, calculated from extrapolated solubility data of Sunier and Baumbach [1] is given alongside the corresponding temperature.

only one known study recording no significant difference between filtered and unfiltered solutions (as discussed in Section 2.2.1). Some other features of the results, such as the apparent increase in the power threshold for laser-induced bubble production, are suspicious and suggest there may be more factors inconsistent between the two data sets beyond filtration. Clearly more information is needed to make any conclusions about the filtration effects. From this study alone there was no significant impact found.

Saturation Effects

According to Tables 9.3 and 9.4, NPLIN apparently occurred where the sample droplet was thought to be undersaturated ($S < 1$). This discrepancy is very likely due to the gradual evaporation of the sample droplet at higher temperatures, increasing the effective saturation of the droplet beyond the stated value, as crystal growth would be prohibited

in an actual undersaturated condition. In these cases, the crystals generated were found to persist as the water continued to evaporate, leaving dry crystals behind on the microscope slides. This identifies an issue with the experimental set-up: the saturation values were clearly not accurate in all cases. In order to avoid this in future, a new droplet could be used for each experiment (very laborious)* or the set-up could be optimised to seal the droplet more effectively, to suppress evaporation.

For the comparison of the filtered and unfiltered samples, it is also worth noting that the concentration of KCl is slightly reduced in the case of Table 9.4, where $C = 0.188$ g KCl/g D_2O, compared with Table 9.3, where $C = 0.190$ g KCl/g D_2O. However, such a small difference would not be expected to significantly impact the threshold for laser-induced bubble formation, so there is likely to be some other unidentified factor differing between the two sets of experiments.

No obvious changes were made to the set up in the interval between recording the results of Table 9.3 and Table 9.4 that would explain the apparent increase in stability with respect to NPLIN and reduced bubble formation at 25%. Though, small changes to the delicate optical set-up which may have impacted the beam reaching the sample, could not be completely ruled out. For any continuation of these experiments, the power reaching the sample should be continuously measured throughout to ensure consistency.

Thoughts on Mechanism and Power Threshold

NPLIN, in this case, was not thought to occur by the trapping mechanism described for CW and femtosecond studies on glycine and lysozyme solutions. Crystallisation occurred rapidly with no evidence for prior aggregation using phase contrast microscopy. On top of this, there was no apparent advantage of focusing the laser at a given interface, as in previous studies, where arranging solute structures may be aided.

From the results presented in Table 9.3, it appears as though there is a power threshold for larger and persisting vapour bubbles, as no bubbles are observed with irradiation at 20% but 12/21 runs produced bubbles at 25%. According to Table 9.2, and considering the power reaching the droplet will be just slightly lower than that measured pre-objective, the range for this apparent threshold corresponds to approximately 0.8 W – 1 W actually reaching the sample droplet.

*For the experiments presented here, a single sample droplet was used and irradiated multiple times at different temperature and power settings while no irradiation effects were visible (i.e. for a series of X results). Until a bubble or crystal was induced to form in the droplet, at which point it was replaced with a new sample droplet of the same solution to continue the testing, the droplet was considered to be unaffected.

The appearance of bubbles in the sample droplets was generally very obvious, in contrast to the crystals which in some cases have very thin edges and take many different forms, visible vapour bubbles of different sizes were always clearly and quickly identifiable by a thick black circle. They are visible even out of focus, as in Figure 9.6, which shows three small bubbles and some KCl crystals alongside each other. It is evident that where a C result was recorded no visible bubbles were formed.

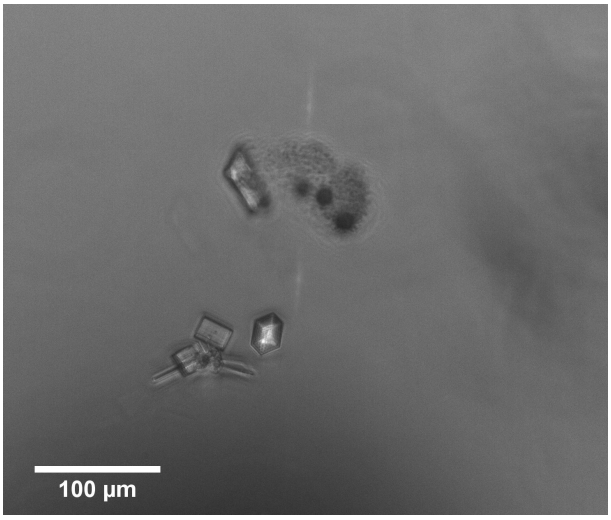

Figure 9.6: KCl crystals and bubbles in solution formed by laser irradiation and vertical focusing. Image shows visual distinction between crystals and bubbles and laser reflection.

In highly supersaturated solutions, crystals may form heterogeneously on larger bubble surfaces. There are two cases of this indicated in Tables 9.3 and 9.4 as BC. The origin of the laser absorption resulting in localised heating and formation of bubbles is not known. It is clear from these observations that heterogeneous crystal nucleation will occur on the surface of a laser generated bubble in a supersaturated solution – as may have been expected. However, it is not yet obvious whether something related can occur at a smaller scale at lower laser powers.

Laser powers below the threshold for the generation of bubbles were found to induce crystallisation quite sporadically and without the apparent appearance of bubbles. It is possible that collapsing bubbles, too small to be seen, are produced at lower powers and crystallisation subsequently occurs either by induced concentration or pressure gradients.

The impact of nanoscale impurities and dust particles (outlined for the nanoparticle heating mechanism in Section 2.2.1) could have better explained the variation in irradiation-time and location for NPLIN observed, as well as the laser absorption. However, filtration was not found to substantially impact the probability for nucleation, maintaining the

mystery of the physical basis for these observations.

Overall, these experiments confirm NPLIN in supersatured KCl/D_2O solutions by 1030 nm femtosecond-pulsed laser irradiation. Recording of laser-induced bubbles at higher powers suggests a possible correlation between this phenomena and NPLIN, as observed for other compounds. The nature of this possible correlation – whether it underlies the mechanism for the laser-induced crystallisation recorded – remains unclear.

Chapter 10

Conclusion

Through a comprehensive literature review on NPLIN phenomenon in KCl, glycine and lysozyme, various approaches to understanding the mechanism underlying NPLIN have been examined. Despite early interpretations [14], a mechanism based on the optical alignment of clusters in *nanosecond-pulsed* NPLIN now seems unlikely. Energetic inconsistencies with the original OKE based mechanism have since been highlighted [28]; and the suspected correlation between crystal orientation and laser alignment could not be identified in later work [27]. The main support for such a mechanism was the reported polarisation switching of glycine crystal polymorphs [67], seeming to suggest a structural re-ordering of clusters by laser light. Yet, attempts to replicate this effect have been unsuccessful [30] [65], casting doubt on the previous results. Further to this, a dielectric polarisation mechanism fails to explain the power thresholds for NPLIN that have now been extensively observed [15] [45] [75] [76].

In the literature, nanosecond and femtosecond/CW NPLIN studies are generally considered distinctly and it is reasonable to assume the two may occur by different mechanisms. However, given that neither mechanism is well understood, it is valuable to contrast the results. Although laser trapping would only occur in the femtosecond/CW case, the incidence of laser-induced bubble formation has been observed for various pulse rates [32] [33] [75].

There is now considerable evidence to suggest that the formation of transient nanobubbles may prelude nucleation in NPLIN. It is thought that the formation and collapse of vapour bubbles may induce pressure or concentration gradients sufficient to facilitate crystal growth. Though, essentially all detail of this mechanism – the method for laser generation of bubbles and nature of the nucleation process – remains unclear. The significance of dust or impurity particles in this mechanism has been proposed [66] [16], but experimental

results have not yet achieved complete consensus on their role.

In previous studies, there have been some clear indications of laser trapping crystallisation, such as transient crystallisation in undersaturated solution [41], CW polarisation effects on glycine polymorphism [34] and the detection of high-concentration regions in the laser focus [36]. The investigation of laser-induced separation of liquid phases is also a promising new approach to illuminate the potential role of liquid-liquid separation in laser trapping NPLIN [25]. Overall, the literature on laser trapping crystallisation to date lacks the consistency to resolve the issue. For example, contrasting studies have suggested NPLIN occurs *exclusively* at the air/solution interface [41] and then more recently at the glass/solution interface [79]. Considering the disparity within the literature on the subject, it seems probable that multiple NPLIN mechanisms may exist. The conditions determining the prevailing mechanism in any case have yet to be identified.

Experimentally, it has been shown that KCl crystal nucleation can be induced by a femtosecond pulse train from D_2O solution. This NPLIN was apparently promoted with translation of the laser focus through the solution, rather than enhanced at a specific position or droplet interface. It was also established that femtosecond laser irradiation of KCl/D_2O solution can lead to the formation of bubbles, above an apparent power threshold (estimated to be in the range 0.8 W – 1 W). This result echoes recent observations of CW/femtosecond NPLIN studies for other compounds [33] [77] [75]; though the origin of the absorption has not yet been identified.

Examining the experimental results in the context of proposed mechanisms for NPLIN, no single mechanism is found to align completely with our observations. In particular, no evidence to support the laser trapping mechanism for femtosecond NPLIN of KCl has been demonstrated.

In some cases, under highly supersaturated conditions, KCl crystals were observed to form heterogeneously on laser-induced bubble surfaces. The link between bubble and crystal formation could indicate the formation of transient nano- or micro-bubbles at lower powers capable of inducing NPLIN in KCl. For the most part, where crystals were generated in our own experiments, no bubbles were visible. In contrast to the emergent threshold for laser-induced bubble formation, no such threshold for NPLIN was obvious. Frequently, crystallisation was induced at powers *below* the bubble threshold. Hence, the relationship between the mechanisms for bubble and crystal formation is still unclear; despite the confirmation that continuous 1030 nm femtosecond irradiation can induce the formation of both. Given how sporadically laser-induced crystallisation was found to occur, a broader study involving more repeated experiments would be appropriate to achieve greater insight into any meaningful trends.

It has also been suggested that a power threshold for laser-induced bubbles may be consistent with a temperature threshold for solvent evaporation based on the laser heating of impurity particles [16]. Yet, the filtration and avoidance of dust were not found to suppress NPLIN in our own limited study, so crediting this particular mechanism would not be justified here despite its feasibility.

Clearly, there is still much to be explored in the search for understanding of NPLIN phenomena. Throughout this report, key areas demanding further study have been highlighted. In particular, using the experimental set-up outlined, it would be valuable to repeat experiments in order to more accurately identify the power threshold observed. It would also be interesting to optimise the experimental set-up and solution composition, to fully investigate NPLIN of glycine and lysozyme solutions – comparing the results with those reported here for KCl. In a broader sense, further investigation into the cause of laser absorption leading to vapour bubbles in D_2O solutions is essential to progress towards greater control over crystal nucleation.

Appendix A

Acetate Buffer Calculation

Required **1 ml of 0.1 M acetate buffer, pH = 4.5**

Using the Henderson-Hasselbalch Equation:

$$pH = pKa + log_{10}\left(\frac{[\text{sodium acetate}]}{[\text{acetic acid}]}\right)$$

For a buffer with pH = 4.5, where the pKa of acetic acid is 4.77 $\implies$

$$\frac{[\text{sodium acetate}]}{[\text{acetic acid}]} = 0.549$$

The overall concentration required is 0.1 M $\implies$

$$[\text{sodium acetate}] + [\text{acetic acid}] = 0.1$$

Combining these, the required concentrations are:

$$[\text{sodium acetate}] = 0.035\, mol\, l^{-1}$$

$$[\text{acetic acid}] = 0.065\, mol\, l^{-1}$$

The masses of each required to produce 1 ml of 0.1 M pH = 4.5 buffer solution therefore are:

Sodium Acetate
FM = 82.03 g mol^{-1}
c = 0.035 mol l^{-1}
v = 1 ml = 0.001 l
$n = c \times v \implies n = 3.5 \times 10^{-4}$ mol
$m = n \times FM \implies \mathbf{m = 0.0287\ g}$

Acetic Acid
FM = 60.052 g mol^{-1}
c = 0.065 mol l^{-1}
v = 1 ml = 0.001 l
$\implies n = 6.5 \times 10^{-4}$ mol
$\implies \mathbf{m = 0.0390\ g}$ ($\approx 37\,\mu l$)

The acidic correction for pD is:

$$pD = pHa + 0.41$$

Where pHa is the apparent reading from the pH meter.

Bibliography

[1] Arthur A Sunier and James Baumbach. The solubility of potassium chloride in ordinary and heavy water. *Journal of Chemical and Engineering Data*, 21(3):335–336, 1976.

[2] David R Lide. *CRC handbook of chemistry and physics: a ready-reference book of chemical and physical data*. CRC press, 1995.

[3] M Jelińska-Kazimierczuk and J Szydłowski. Isotope effect on the solubility of amino acids in water. *Journal of solution chemistry*, 25(12):1175–1184, 1996.

[4] BJ Murray, JF Ross, TF Whale, HC Price, JD Atkinson, NS Umo, ME Webb, et al. The relevance of nanoscale biological fragments for ice nucleation in clouds. *Scientific reports*, 5:8082, 2015.

[5] Christopher B Marshall, Garth L Fletcher, and Peter L Davies. Hyperactive antifreeze protein in a fish. *Nature*, 429(6988):153–153, 2004.

[6] Richard Sear. What do crystals nucleate on? what is the microscopic mechanism? how can we model nucleation? *MRS Bulletin*, 41(5):363–368, 2016.

[7] J Willard Gibbs. The scientific paper of J. Williard Gibbs. *Thermodynamics*, 1:55, 1961.

[8] Martin Volmer and A Weber. Keimbildung in übersättigten gebilden. *Zeitschrift für physikalische Chemie*, 119(1):277–301, 1926.

[9] Richard Becker and Werner Döring. Kinetische behandlung der keimbildung in übersättigten dämpfen. *Annalen der Physik*, 416(8):719–752, 1935.

[10] Julius Frenkel. A general theory of heterophase fluctuations and pretransition phenomena. *The Journal of Chemical Physics*, 7(7):538–547, 1939.

[11] Pieter Rein ten Wolde and Daan Frenkel. Homogeneous nucleation and the Ostwald step rule. *Physical Chemistry Chemical Physics*, 1(9):2191–2196, 1999.

[12] Andrew J Alexander and Philip J Camp. Non-photochemical laser-induced nucleation. *The Journal of chemical physics*, 150(4):040901, 2019.

[13] John Tyndall. On the blue color of the sky, the polarization of skylight, and polarization of light by cloudy matter generally. *Journal of the Franklin Institute*, 88(1):34–40, 1869.

[14] BA Garetz, JE Aber, NL Goddard, RG Young, and AS Myerson. Nonphotochemical, polarization-dependent, laser-induced nucleation in supersaturated aqueous urea solutions. *Physical review letters*, 77(16):3475, 1996.

[15] Andrew J Alexander and Philip J Camp. Single pulse, single crystal laser-induced nucleation of potassium chloride. *Crystal Growth and Design*, 9(2):958–963, 2009.

[16] Martin R Ward, Alasdair M Mackenzie, and Andrew J Alexander. Role of impurity nanoparticles in laser-induced nucleation of ammonium chloride. *Crystal Growth & Design*, 16(12):6790–6796, 2016.

[17] Martin R Ward, Gary W Copeland, and Andrew J Alexander. Chiral hide-and-seek: Retention of enantiomorphism in laser-induced nucleation of molten sodium chlorate. *The Journal of chemical physics*, 135(11):114508, 2011.

[18] Martin R Ward, Stephanie McHugh, and Andrew J Alexander. Non-photochemical laser-induced nucleation of supercooled glacial acetic acid. *Physical Chemistry Chemical Physics*, 14(1):90–93, 2012.

[19] Julien Zaccaro, Jelena Matic, Allan S Myerson, and Bruce A Garetz. Nonphotochemical, laser-induced nucleation of supersaturated aqueous glycine produces unexpected γ-polymorph. *Crystal Growth & Design*, 1(1):5–8, 2001.

[20] Arthur Ashkin. Acceleration and trapping of particles by radiation pressure. *Physical review letters*, 24(4):156, 1970.

[21] B Agate, CTA Brown, W Sibbett, and K Dholakia. Femtosecond optical tweezers for in-situ control of two-photon fluorescence. *Optics Express*, 12(13):3011–3017, 2004.

[22] Masayasu Muramatsu, Tse-Fu Shen, Wei-Yi Chiang, Anwar Usman, and Hiroshi Masuhara. Picosecond motional relaxation of nanoparticles in femtosecond laser trapping. *The Journal of Physical Chemistry C*, 120(9):5251–5256, 2016.

[23] Pieter Rein ten Wolde and Daan Frenkel. Enhancement of protein crystal nucleation by critical density fluctuations. *Science*, 277(5334):1975–1978, 1997.

[24] Jan Wedekind, Limei Xu, Sergey V Buldyrev, H Eugene Stanley, David Reguera, and Giancarlo Franzese. Optimization of crystal nucleation close to a metastable fluid-fluid phase transition. *Scientific reports*, 5:11260, 2015.

[25] Finlay Walton and Klaas Wynne. Control over phase separation and nucleation using a laser-tweezing potential. *Nature chemistry*, 10(5):506–510, 2018.

[26] Finlay Walton and Klaas Wynne. Using optical tweezing to control phase separation and nucleation near a liquid–liquid critical point. *Soft matter*, 15(41):8279–8289, 2019.

[27] Yao Liu, Martin R Ward, and Andrew J Alexander. Polarization independence of laser-induced nucleation in supersaturated aqueous urea solutions. *Physical Chemistry Chemical Physics*, 19(5):3464–3467, 2017.

[28] Brandon C Knott, Michael F Doherty, and Baron Peters. A simulation test of the optical kerr mechanism for laser-induced nucleation. *The Journal of chemical physics*, 134(15):154501, 2011.

[29] Martin R Ward, Alasdair Rae, and Andrew J Alexander. Nonphotochemical laser-induced crystal nucleation by an evanescent wave. *Crystal Growth & Design*, 15(9):4600–4605, 2015.

[30] Yao Liu, Mees H van den Berg, and Andrew J Alexander. Supersaturation dependence of glycine polymorphism using laser-induced nucleation, sonocrystallization and nucleation by mechanical shock. *Physical Chemistry Chemical Physics*, 19(29):19386–19392, 2017.

[31] Brandon C Knott, Jerry L Larue, Alec M Wodtke, Michael F Doherty, and Baron G Peters. Communication: Bubbles, crystals, and laser-induced nucleation. *Journal of Chemical Physics*, 134(17):171102, 2011.

[32] Martin R Ward, William J Jamieson, Claire A Leckey, and Andrew J Alexander. Laser-induced nucleation of carbon dioxide bubbles. *The Journal of chemical physics*, 142(14):144501, 2015.

[33] Kazuhiko Nakamura, Yoichiroh Hosokawa, and Hiroshi Masuhara. Anthracene crystallization induced by single-shot femtosecond laser irradiation: experimental evidence for the important role of bubbles. *Crystal growth & design*, 7(5):885–889, 2007.

[34] Ken-ichi Yuyama, Thitiporn Rungsimanon, Teruki Sugiyama, and Hiroshi Masuhara. Selective fabrication of α-and γ-polymorphs of glycine by intense polarized continuous wave laser beams. *Crystal growth & design*, 12(5):2427–2434, 2012.

[35] Hiroaki Adachi, Kazufumi Takano, Youichiroh Hosokawa, Tsuyoshi Inoue, Yusuke Mori, Hiroyoshi Matsumura, Masashi Yoshimura, Yasuo Tsunaka, Masaaki Morikawa, Shigenori Kanaya, et al. Laser irradiated growth of protein crystal. *Japanese journal of applied physics*, 42(7B):L798, 2003.

[36] Yasuyuki Tsuboi, Tatsuya Shoji, and Noboru Kitamura. Crystallization of lysozyme based on molecular assembling by photon pressure. *Japanese Journal of Applied Physics*, 46(12L):L1234, 2007.

[37] In Sung Lee, James MB Evans, Deniz Erdemir, Alfred Y Lee, Bruce A Garetz, and Allan S Myerson. Nonphotochemical laser induced nucleation of hen egg white lysozyme crystals. *Crystal Growth and Design*, 8(12):4255–4261, 2008.

[38] Teruki Sugiyama, Takuji Adachi, and Hiroshi Masuhara. Crystallization of glycine by photon pressure of a focused CW laser beam. *Chemistry letters*, 36(12):1480–1481, 2007.

[39] Teruki Sugiyama, Takuji Adachi, and Hiroshi Masuhara. Crystal growth of glycine controlled by a focused CW near-infrared laser beam. *Chemistry letters*, 38(5):482–483, 2009.

[40] Thitiporn Rungsimanon, Ken-ichi Yuyama, Teruki Sugiyama, Hiroshi Masuhara, Norimitsu Tohnai, and Mikiji Miyata. Control of crystal polymorph of glycine by photon pressure of a focused continuous wave near-infrared laser beam. *The Journal of Physical Chemistry Letters*, 1(3):599–603, 2010.

[41] Thitiporn Rungsimanon, Ken-ichi Yuyama, Teruki Sugiyama, and Hiroshi Masuhara. Crystallization in unsaturated glycine/D2O solution achieved by irradiating a focused continuous wave near infrared laser. *Crystal growth & design*, 10(11):4686–4688, 2010.

[42] Jing-Ru Tu, Ken-ichi Yuyama, Hiroshi Masuhara, and Teruki Sugiyama. Dynamics and mechanism of laser trapping-induced crystal growth of hen egg white lysozyme. *Crystal Growth & Design*, 15(10):4760–4767, 2015.

[43] Ke Fang, Stephen Arnold, and Bruce A Garetz. Nonphotochemical laser-induced nucleation in levitated supersaturated aqueous potassium chloride microdroplets. *Crystal growth & design*, 14(5):2685–2688, 2014.

[44] Carla Duffus, Philip J Camp, and Andrew J Alexander. Spatial control of crystal nucleation in agarose gel. *Journal of the American Chemical Society*, 131(33):11676–11677, 2009.

[45] Tianyi Hua, Omar Gowayed, Danielle Grey-Stewart, Bruce A Garetz, and Ryan L Hartman. Microfluidic laser-induced nucleation of supersaturated aqueous KCl solutions. *Crystal Growth & Design*, 19(6):3491–3497, 2019.

[46] Martin R Ward and Andrew J Alexander. Nonphotochemical laser-induced nucleation of potassium halides: Effects of wavelength and temperature. *Crystal growth & design*, 12(9):4554–4561, 2012.

[47] Jelena Matic, Xiaoying Sun, Bruce A Garetz, and Allan S Myerson. Intensity, wavelength, and polarization dependence of nonphotochemical laser-induced nucleation in supersaturated aqueous urea solutions. *Crystal growth & design*, 5(4):1565–1567, 2005.

[48] Rohit Kacker, Sanjana Dhingra, Daniel Irimia, Murali Krishna Ghatkesar, Andrzej Stankiewicz, Herman JM Kramer, and Huseyin Burak Eral. Multiparameter investigation of laser-induced nucleation of supersaturated aqueous KCl solutions. *Crystal Growth & Design*, 18(1):312–317, 2018.

[49] YC Chang and AS Myerson. The diffusivity of potassium chloride and sodium chloride in concentrated, saturated, and supersaturated aqueous solutions. *AIChE journal*, 31(6):890–894, 1985.

[50] Julien O Sindt, Andrew J Alexander, and Philip J Camp. Structure and dynamics of potassium chloride in aqueous solution. *The Journal of Physical Chemistry B*, 118(31):9404–9413, 2014.

[51] Martin R Ward, Iain Ballingall, Matthew L Costen, Kenneth G McKendrick, and Andrew J Alexander. Nanosecond pulse width dependence of nonphotochemical laser-induced nucleation of potassium chloride. *Chemical Physics Letters*, 481(1-3):25–28, 2009.

[52] SV Goryainov, EV Boldyreva, and EN Kolesnik. Raman observation of a new (ζ) polymorph of glycine? *Chemical Physics Letters*, 419(4-6):496–500, 2006.

[53] Alice Dawson, David R Allan, Scott A Belmonte, Stewart J Clark, William IF David, Pamela A McGregor, Simon Parsons, Colin R Pulham, and Lindsay Sawyer. Effect of high pressure on the crystal structures of polymorphs of glycine. *Crystal growth & design*, 5(4):1415–1427, 2005.

[54] Andréanne Bouchard, Gerard W Hofland, and Geert-Jan Witkamp. Solubility of glycine polymorphs and recrystallization of β-glycine. *Journal of Chemical & Engineering Data*, 52(5):1626–1629, 2007.

[55] Eun Hee Lee. A practical guide to pharmaceutical polymorph screening & selection. *asian journal of pharmaceutical sciences*, 9(4):163–175, 2014.

[56] K Raza, P Kumar, S Ratan, R Malik, and S Arora. Polymorphism: The phenomenon affecting the performance of drugs. *SOJ Pharm Pharm Sci,*, 1(2):1–10, 2014.

[57] Jack D Dunitz and Joel Bernstein. Disappearing polymorphs. *Accounts of chemical research*, 28(4):193–200, 1995.

[58] EV Boldyreva, VA Drebushchak, TN Drebushchak, IE Paukov, Yu A Kovalevskaya, and ES Shutova. Polymorphism of glycine, Part I. *Journal of thermal analysis and calorimetry*, 73(2):409–418, 2003.

[59] Colan E Hughes and Kenneth DM Harris. The effect of deuteration on polymorphic outcome in the crystallization of glycine from aqueous solution. *New Journal of Chemistry*, 33(4):713–716, 2009.

[60] Encyclopædia Britannica. Polymorphism. `https://www.britannica.com/science/polymorphism-crystals`, May 2009.

[61] Yoichi Iitaka. The crystal structure of γ-glycine. *Acta Crystallographica*, 14(1):1–10, 1961.

[62] Wilhelm Ostwald. Studien über die bildung und umwandlung fester körper. *Zeitschrift für physikalische Chemie*, 22(1):289–330, 1897.

[63] Terry Threlfall. Structural and thermodynamic explanations of Ostwald's rule. *Organic process research & development*, 7(6):1017–1027, 2003.

[64] Xiaoying Sun, Bruce A Garetz, and Allan S Myerson. Supersaturation and polarization dependence of polymorph control in the nonphotochemical laser-induced nucleation (NPLIN) of aqueous glycine solutions. *Crystal growth & design*, 6(3):684–689, 2006.

[65] Bertrand Clair, Aziza Ikni, Wenjing Li, Philippe Scouflaire, Vincent Quemener, and Anne Spasojević-de Biré. A new experimental setup for high-throughput controlled non-photochemical laser-induced nucleation: application to glycine crystallization. *Journal of Applied Crystallography*, 47(4):1252–1260, 2014.

[66] Nadeem Javid, Thomas Kendall, Iain S Burns, and Jan Sefcik. Filtration suppresses laser-induced nucleation of glycine in aqueous solutions. *Crystal Growth & Design*, 16(8):4196–4202, 2016.

[67] Bruce A Garetz, Jelena Matic, and Allan S Myerson. Polarization switching of crystal structure in the nonphotochemical light-induced nucleation of supersaturated aqueous glycine solutions. *Physical review letters*, 89(17):175501, 2002.

[68] Xiaoying Sun, Bruce A Garetz, and Allan S Myerson. Polarization switching of crystal structure in the nonphotochemical laser-induced nucleation of supersaturated aqueous L-histidine. *Crystal Growth and Design*, 8(5):1720–1722, 2008.

[69] JA Littlechild. Protein crystallization: magical or logical: can we establish some general rules? *Journal of Physics D: Applied Physics*, 24(2):111, 1991.

[70] Martin Muschol and Franz Rosenberger. Liquid–liquid phase separation in supersaturated lysozyme solutions and associated precipitate formation/crystallization. *The Journal of chemical physics*, 107(6):1953–1962, 1997.

[71] Biological Magnetic Resonance Data Bank. BMRB featured system: Lysozyme. `http://www.bmrb.wisc.edu/featuredSys/Lysozyme/`, January 2017.

[72] Sathyadevi Venkataramani, Jeremy Truntzer, and Denis R Coleman. Thermal stability of high concentration lysozyme across varying pH: A fourier transform infrared study. *Journal of pharmacy & bioallied sciences*, 5(2):148, 2013.

[73] Oleg Galkin and Peter G Vekilov. Control of protein crystal nucleation around the metastable liquid–liquid phase boundary. *Proceedings of the National Academy of Sciences*, 97(12):6277–6281, 2000.

[74] Oleg Galkin and Peter G Vekilov. Are nucleation kinetics of protein crystals similar to those of liquid droplets? *Journal of the American chemical society*, 122(1):156–163, 2000.

[75] Hiroshi Y Yoshikawa, Ryota Murai, Syou Maki, Tomoya Kitatani, Shigeru Sugiyama, Gen Sazaki, Hiroaki Adachi, Tsuyoshi Inoue, Hiroyoshi Matsumura, Kazufumi Takano, et al. Laser energy dependence on femtosecond laser-induced nucleation of protein. *Applied Physics A*, 93(4):911–915, 2008.

[76] Ryota Murai, Hiroshi Y Yoshikawa, Hitoshi Hasenaka, Yoshinori Takahashi, Mihoko Maruyama, Shigeru Sugiyama, Hiroaki Adachi, Kazufumi Takano, Hiroyoshi Matsumura, Satoshi Murakami, et al. Influence of energy and wavelength on femtosecond laser-induced nucleation of protein. *Chemical Physics Letters*, 510(1-3):139–142, 2011.

[77] Natsuko Iefuji, Ryota Murai, Mihoko Maruyama, Yoshinori Takahashi, Shigeru Sugiyama, Hiroaki Adachi, Hiroyoshi Matsumura, Satoshi Murakami, Tsuyoshi Inoue, Yusuke Mori, et al. Laser-induced nucleation in protein crystallization: Local increase

in protein concentration induced by femtosecond laser irradiation. *Journal of crystal growth*, 318(1):741–744, 2011.

[78] Jing-Ru Tu, Atsushi Miura, Ken-ichi Yuyama, Hiroshi Masuhara, and Teruki Sugiyama. Crystal growth of lysozyme controlled by laser trapping. *Crystal growth & design*, 14(1):15–22, 2014.

[79] Ken-ichi Yuyama, Kai-Di Chang, Jing-Ru Tu, Hiroshi Masuhara, and Teruki Sugiyama. Rapid localized crystallization of lysozyme by laser trapping. *Physical Chemistry Chemical Physics*, 20(9):6034–6039, 2018.

[80] Martin F Chaplin. Water's hydrogen bond strength. *Water and Life: The unique properties of H2O*, pages 69–86, 2010.

[81] Allan S Myerson and Pei Yi Lo. Diffusion and cluster formation in supersaturated solutions. *Journal of Crystal Growth*, 99(1-4):1048–1052, 1990.

[82] LS Sorell and AS Myerson. Diffusivity of urea in concentrated, saturated and supersaturated solutions. *AIChE journal*, 28(5):772–779, 1982.

[83] Yeong-Chul Kim and Allan S Myerson. Diffusivity of lysozyme in undersaturated, saturated and supersaturated solutions. *Journal of crystal growth*, 143(1-2):79–85, 1994.

[84] Omar Gowayed, Tasfia Tasnim, José J Fuentes-Rivera, Janice E Aber, and Bruce A Garetz. Non-photochemical pulsed-laser-induced nucleation in a continuous-wave-laser-induced phase-separated solution droplet of aqueous glycine formed by optical gradient forces. *Crystal Growth & Design*, 19(12):7372–7379, 2019.

[85] WC Waggener. Absorbance of liquid water and deuterium oxide between 0.6 and 1.8 microns. Comparison of absorbance and effect of temperature. *Analytical Chemistry*, 30(9):1569–1570, 1958.

[86] JG Bayly, VB Kartha, and WH Stevens. The absorption spectra of liquid phase H2O, HDO and D2O from 0· 7 μm to 10 μm. *Infrared Physics*, 3(4):211–222, 1963.